Frontiers in Bioscience Landmark

Front. Biosci. (Landmark Ed) **2025**; 30(10): 45558
https://doi.org/10.31083/FBL45558

Original Research

Metabolomics Profiling of Kidney, Spleen, Lung, and Liver Tissues in a Mouse Model of Sepsis

Moongi Ji[1,†], Byeongchan Choi[1,†], Chanho Kim[1], Jaeyeop Lim[1], Man-Jeong Paik[1,*]

[1]College of Pharmacy and Research Institute of Life and Pharmaceutical Sciences, Sunchon National University, 57922 Suncheon, Republic of Korea
*Correspondence: paik815@scnu.ac.kr (Man-Jeong Paik)
[†]These authors contributed equally.

Academic Editor: Francesco Gavelli
Submitted: 5 August 2025 Revised: 24 September 2025 Accepted: 20 October 2025 Published: 31 October 2025

Abstract

Background: Sepsis is a life-threatening condition characterized by a dysregulated host response to infection, often leading to multiorgan dysfunction. Despite their clinical importance, early diagnostic biomarkers that reflect organ-specific damage remain inadequately characterized. **Methods**: Targeted metabolomic profiling of amino acids, organic acids, fatty acids, nucleosides, and kynurenine pathway metabolites was performed on lung, kidney, spleen, and liver tissues obtained from a lipopolysaccharide-induced mouse model of sepsis, using liquid chromatography-tandem mass spectrometry and gas chromatography-tandem mass spectrometry. Univariate and multivariate statistical analyses (principal component analysis and partial least squares discriminant analysis) were performed to identify potential biomarkers, followed by pathway analysis to elucidate their biological relevance. **Results**: Twenty-nine metabolites were significantly altered across the four tissues, exhibiting organ-specific metabolic signatures. Tyrosine, epinephrine, 5-hydroxytryptophan, and kynurenic acid in the kidney; serine, 4-hydroxyproline, normetanephrine, xanthosine, uridine, adenosine, succinic acid, *cis*-aconitic acid, linoleic acid, and eicosadienoic acid in the spleen; alanine, α-aminobutyric acid, ornithine, uridine, adenosine, 5′-deoxy-5′-methylthioadenosine, succinic acid, and *cis*-aconitic acid in the lung; and α-aminobutyric acid, pipecolic acid, uridine, inosine, adenosine, glycolic acid, and oxaloacetic acid in the liver were identified as potential biomarkers reflecting organ-specific dysfunction in sepsis. **Conclusions**: This study highlights the distinct organ-specific metabolic alterations in sepsis and identifies candidate biomarkers that may reflect early organ dysfunction. These findings provide a foundation for the development of precise diagnostic and medical strategies for sepsis.

Keywords: sepsis; organ dysfunction; metabolomics; biomarker

1. Introduction

Sepsis is a life-threatening condition characterized by a dysregulated host response to infection, resulting in physiological, pathological, and biochemical disturbances. It often leads to systemic inflammation, oxidative stress, multiple organ dysfunction, septic shock, and death [1,2]. According to a global estimate, in 2017, sepsis accounted for approximately 489,000 cases and 110,000 related deaths, representing 19.7% of the global mortality [3]. Despite advances in medical care and clinical awareness, sepsis remains a major contributor to morbidity and mortality worldwide. The heterogeneous clinical manifestations of sepsis pose significant challenges to its diagnosis and management [4].

Biomarkers reflecting the pathophysiological changes in sepsis have been investigated as potential tools for improving clinical decision-making and patient outcomes. Among these, procalcitonin, C-reactive protein, interleukin-6, presepsin, and CD64 have been proposed as diagnostic markers [5]. However, most recent studies have focused on evaluating individual biomarkers in isolation, which may be insufficient given the multifactorial and dynamic nature of sepsis; thus, ongoing research aims to identify optimal combinations of biomarkers [6–8]. The Sepsis-3 consensus emphasizes the importance of early detection of organ dysfunction as a key determinant of prognosis and therapeutic success [9].

Recent studies have proposed urinary metabolites such as 3-methylhistidine as early biomarkers for sepsis-associated acute kidney injury (SA-AKI) [10,11]. Moreover, metabolic reprogramming in SA-AKI, including impaired fatty acid oxidation and suppression of peroxisome proliferator-activated receptor α [12], underscores the importance of organ-specific metabolomics approaches. Integrated clinical–preclinical investigations and organ-level metabolomics have further revealed that inter-tissue metabolic heterogeneity and mitochondria-related metabolic signatures may precede overt organ dysfunction, with several studies identifying candidate markers of early renal injury [11,13]. Nonetheless, a comprehensive understanding of tissue-level metabolic alterations in sepsis remains limited. Metabolomics, also known as metabolic profiling or phenotyping, is a powerful systems biology approach that comprehensively captures metabolic changes in biological samples in response to physiological stress, environmental stimuli, and disease states [14]. Recent metabolomic studies have enhanced our understanding of sepsis pathogenesis, particularly its hypermetabolic fea-

tures, and have revealed significant perturbations in carbohydrate, protein, and lipid metabolism, as well as alterations in nucleoside (NS) and kynurenine pathway (KP) metabolites, especially in severe cases [15–17]. Identifying organ-specific metabolic signatures through targeted metabolomic profiling may provide a more sensitive and earlier indication of impending organ dysfunction than conventional clinical assessments. These insights may facilitate the development of timely interventions and therapeutic strategies. Therefore, this study aimed to identify diagnostic biomarkers and elucidate key metabolic pathways associated with sepsis-induced organ dysfunction by performing targeted metabolomic profiling of amino acids (AAs), organic acids (OAs), fatty acids (FAs), NSs, and KP metabolites, followed by multivariate statistical and pathway enrichment analyses in kidney, spleen, lung, and liver tissues.

2. Materials and Methods

2.1 Chemicals and Standards

The standards, including 31 AAs (alanine, methionine, phenylalanine, cysteine, proline, aspartic acid, glycine, valine, glutamic acid, serine, asparagine, leucine, isoleucine, glutamine, threonine, lysine, histidine, tyrosine, tryptophan, α-aminobutyric acid, N-acetylleucine, N-acetylisoleucine, β-aminoisobutyric acid, γ-aminobutyric acid, homocysteine, ornithine, pipecolic acid, pyroglutamic acid, α-aminoadipic acid, 4-hydroxyproline, and N-methyl-DL-aspartic acid), 17 OAs (pyruvic acid, acetoacetic acid, lactic acid, glycolic acid, 2-hydroxybutyric acid, 3-hydroxybutyric acid, malonic acid, succinic acid, fumaric acid, oxaloacetic acid, α-ketoglutaric acid, 4-hydroxyphenylacetic acid, malic acid, 2-hydroxyglutaric acid, *cis*-aconitic acid, 4-hydroxyphenyllactic acid, and citric acid), 17 FAs (myristic acid, palmitoleic acid, palmitic acid, linoleic acid, oleic acid, α-linolenic acid, stearic acid, arachidonic acid, gondoic acid, eicosadienoic acid, arachidic acid, docosahexaenoic acid, adrenic acid, behenic acid, nervonic acid, lignoceric acid, and cerotic acid), 13 NSs (5,6-dihydrouridine, pseudouridine, cytidine, 5-methylcytidine, uridine, inosine, guanosine, xanthosine, 1-methylguanosine, N^2-methylguanosine, adenosine, N^2,N^2-dimethylguanosine, and 5′-deoxy-5′-methylthioadenosine (MTA)), and 10 KPs (picolinic acid, 5-hydroxytryptophan, kynurenine, xanthurenic acid, kynurenic acid, anthranilic acid, epinephrine, normetanephrine, DOPA, and serotonin) were purchased from Sigma-Aldrich (St. Louis, MO, USA) and Tokyo Chemical Industry (Kita-ku, Tokyo, Japan). Internal standards (ISs), including norvaline, $^{13}C_2$-succinic acid, 3,4-dimethoxybenzoic acid, pentadecanoic acid, and 3-deazauridine, were obtained from Sigma-Aldrich (St. Louis, MO, USA). All standard mixtures and ISs were stored at –20 °C until use.

2.2 Animal Model

The animal model used in this study (n = 5) was derived from the referenced article [18]. Six week-old female BALB/c mice (about 20 g) were purchased from Orient Bio (Daejeon, Korea) and housed under pathogen-free conditions with controlled temperature and humidity for at least 1 week before experimentation. To establish the mice model, lipopolysaccharide (LPS, 20 mg·kg^{-1}) dissolved in phosphate-buffered saline (PBS) was administered intraperitoneally, whereas the control group received intraperitoneal injections of PBS alone. Euthanasia was performed in a chamber of approximately 10 L volume, into which 100% CO_2 was introduced at a displacement rate of 30–70% of the chamber volume per minute (3–7 L/min). Unconsciousness was typically observed within 2–3 minutes, and CO_2 exposure was maintained for a total of ~5 minutes to ensure irreversible euthanasia. The tissues were collected at the time of sacrifice, 6 hours after LPS administration, and each experimental group. Animal care and experimental procedures followed the ARRIVE guidelines as well as the institutional guidelines approved by the Institutional Animal Care and Use Committee (IACUC) of Konkuk University (approval no. KU17044-2) [18].

2.3 Gas Chromatography-tandem Mass Spectrometry

Gas chromatography-tandem mass spectrometry (GC–MS/MS) analysis was performed using a Shimadzu TQ 8040 triple-quadrupole mass spectrometer (Shimadzu, Kyoto, Japan). Metabolite separation was achieved with a cross-linked Ultra-2 capillary column (25 m × 0.20 mm I.D., 0.11 µm film thickness; 5% phenyl–95% methylpolysiloxane stationary phase) (Agilent Technologies, Palo Alto, CA, USA). A 1.0 µL aliquot of each sample was introduced via split injection at a ratio of 10:1. For the profiling of AAs, Oas, and FAs, the GC oven temperature was programmed to start at 100 °C and held for 2 min, followed by a linear ramp of 10 °C/min to 300 °C, which was then maintained for 8 min. Helium was used as the carrier gas at a constant flow rate of 0.5 mL/min, and argon served as the collision gas. Electron impact ionization at 70 eV was used to ionize the target analytes.

2.4 Liquid Chromatography-tandem Mass Spectrometry

Liquid chromatography-tandem mass spectrometry (LC-MS/MS) analysis was performed using a Shimadzu LCMS-8050 triple-quadrupole mass spectrometer (Shimadzu, Kyoto, Japan). Separation of NSs and KP metabolites was achieved using a ZORBAX Eclipse XDB-C18 column measuring 150 mm in length, 4.6 mm in internal diameter, and 5 µm in particle size (Agilent Technologies, Palo Alto, CA, USA). The instrument was operated in the electrospray ionization mode with a nebulizing gas flow rate of 3.0 L/min and a heating gas flow rate of 10.0 L/min. The interface temperature was maintained at 300 °C, and the desolvation line temperature was set to 250 °C. Gradient

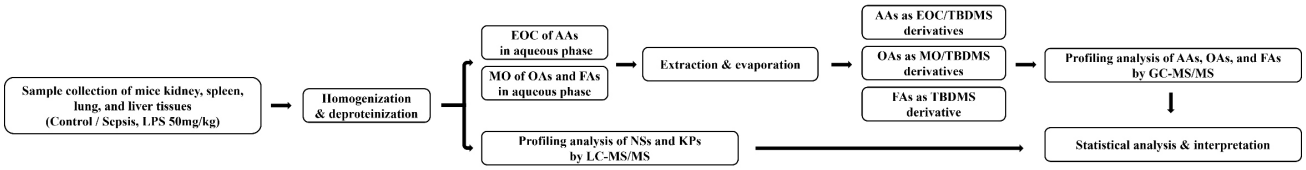

Fig. 1. Flowchart of metabolomics analysis. EOC, ethoxycarbonylation; TBDMS, tert-butyldimethylsilylation; MO, methoximation; LC–MS/MS, Liquid chromatography-tandem mass spectrometry; GC–MS/MS, Gas chromatography-tandem mass spectrometry; AAs, amino acids; OAs, organic acids; FAs, fatty acids; NSs, nucleosides; KPs, Kynurenine pathway metabolites.

elution was implemented for chromatographic separation using 10 mM ammonium acetate as mobile phase A and methanol as mobile phase B for NSs, whereas 0.1% formic acid in water was used as mobile phase A and 0.1% formic acid in acetonitrile as mobile phase B for KP metabolites.

2.5 Sample Preparation for GC–MS/MS-based Profiling of AAs, OAs, and FAs in Tissue Samples From Control and Sepsis Groups

Kidney, spleen, lung, and liver tissues were homogenized in water using an ultrasonicator (VCX-600; Sonics & Materials, Danbury, CT, USA). Supernatants were collected after centrifugation at 13,500 rpm for 5 min at 4 ℃. Profiling analysis of AAs, OAs, and FAs in tissue samples was performed using ethoxycarbonylation (EOC)/tert-butyldimethylsilylation (TBDMS) and methoximation (MO)/TBDMS derivatization, as previously described [19].

For AA analysis, 2 mg of tissue sample was deproteinized by adding 100 µL of acetonitrile containing 0.2 µg of norvaline as an IS. After centrifugation, the resulting supernatant was mixed with 1.0 mL of water and transferred to 2.0 mL of dichloromethane containing ethyl chloroformate (ECF). The pH was adjusted to $\geq$12 using 5 M sodium hydroxide, and amine groups were derivatized via a two-phase EOC reaction by vortexing for 10 min, resulting in the formation of EOC derivatives.

For the analysis of OA and FA, 5 mg of tissue sample was treated with 100 µL of acetonitrile containing internal standards (0.5 µg of $^{13}C_2$-succinic acid, 0.1 µg of 3,4-dimethoxybenzoic acid, and 0.1 µg of pentadecanoic acid). After centrifugation, the supernatant was combined with 1.0 mL of distilled water and 1 mg of methoxyamine hydrochloride. The pH was adjusted to $\geq$12 using 5.0 M sodium hydroxide, and the solution was incubated at 60 °C for 1 h to allow formation of methoxime derivatives. After the EOC or MO reactions, all aqueous solutions were acidified to pH $\leq$2 using 10% sulfuric acid, saturated with sodium chloride, and extracted sequentially with 3.0 mL of diethyl ether and 2.0 mL of ethyl acetate. The organic extracts were evaporated to dryness under a gentle stream of nitrogen at 40 °C. The dried residues were then treated with 10 µL of toluene and 20 µL of MTBSTFA [N-Methyl-N-(tert-butyldimethylsilyl) trifluoroacetamide], followed by incubation at 60 °C for 1 h to form TBDMS derivatives. The final derivatives were analyzed using GC–MS/MS. The steps of metabolomics analysis shown in Fig. 1.

2.6 Sample Preparation for LC–MS/MS-based Profiling of NSs and KP Metabolites in Tissue Samples From Control and Sepsis Groups

Profiling analyses of NSs and KP metabolites in the tissue samples were performed without derivatization using LC–MS/MS. For deproteinization, 2 mg of lung tissue was mixed with 80 µL of acetonitrile containing internal standards (0.5 ng of 3-deazauridine and 500 ng of 3,4-dimethoxybenzoic acid) in an Eppendorf tube and vortexed for 3 min. After centrifugation, the supernatant was filtered and transferred to an autosampler vial for injection into the LC–MS/MS system. The steps of metabolomics analysis shown in Fig. 1.

2.7 Star Pattern Recognition and Statistical Analyses

Quantitative levels of metabolites in the kidney, spleen, lung, and liver tissues were calculated using calibration curves. To visualize the metabolic alterations in the sepsis group, star plots were constructed based on values normalized to the mean of the control group using Microsoft Excel (version 2010; Microsoft Corporation, Redmond, WA, USA). Quantified metabolite data were log-transformed and auto-scaled to ensure comparability across variables. Univariate analysis was performed using the non-parametric Mann–Whitney U test to assess significant differences between groups. Principal component analysis (PCA) and partial least squares discriminant analysis (PLS-DA) were used to evaluate global metabolic patterns and identify discriminative features. The statistical significances of the group patterns are evaluated using PERMANOVA (based on 999 permutations) for validation of the PCA. The PLS-DA models were based on leave-one-out cross validation (LOOCV) method, that statistical significances of the group patterns providing the basis for the computation of the predictive ability (Q^2), determination coefficient (R^2), and the classification accuracy of the model. Pathway enrichment analysis was conducted to explore the biological relevance of altered metabolites. All statistical analyses were performed using MetaboAnalyst 6.0 (https://www.metaboanalyst.ca).

Table 1. Levels of amino acid, organic acid, fatty acid, nucleoside, and kynurenine pathway metabolite in kidney and spleen tissues from the control and sepsis groups.

No.	Metabolite	Amount (ng/mg, mean ± SD)				Normalized value (mean ± SD)[b]		*p*-value[c]	
		Kidney		Spleen					
		Control	Sepsis	Control	Sepsis	Kidney	Spleen	Kidney	Spleen
1	Alanine	463.45 ± 118.13	507.86 ± 32.19	1076.41 ± 292.59	904.05 ± 100.41	1.10 ± 0.07	0.84 ± 0.09	0.690	0.151
2	Glycine	378.72 ± 183.66	466.05 ± 123.61	4278.73 ± 1401.40	2649.68 ± 547.93	1.23 ± 0.33	0.62 ± 0.13	0.310	0.151
3	α-Aminobutyric acid	0.92 ± 0.21	1.00 ± 0.26	1.21 ± 0.13	1.42 ± 0.14	1.09 ± 0.28	1.18 ± 0.12	0.690	0.016
4	Valine	333.56 ± 49.23	343.67 ± 30.71	226.83 ± 22.69	215.83 ± 20.80	1.03 ± 0.09	0.95 ± 0.09	0.690	0.421
5	Leucine	340.93 ± 17.93	359.88 ± 14.08	963.95 ± 214.44	1278.86 ± 121.74	1.06 ± 0.04	1.33 ± 0.13	0.151	0.032
6	Isoleucine	227.47 ± 44.11	243.11 ± 14.16	369.29 ± 90.90	240.58 ± 42.66	1.07 ± 0.06	0.65 ± 0.12	0.841	0.056
7	Proline	688.71 ± 407.14	405.20 ± 88.42	200.02 ± 49.18	193.70 ± 23.72	0.59 ± 0.13	0.97 ± 0.12	0.222	0.548
8	Pipecolic acid	2.55 ± 3.15	0.85 ± 0.42	N.D.[a]	N.D.[a]	0.33 ± 0.16	-	0.310	-
9	Pyroglutamic acid	383.14 ± 349.45	167.66 ± 89.19	87.86 ± 11.61	119.04 ± 47.77	0.44 ± 0.23	0.82 ± 0.15	0.310	0.151
10	Methionine	164.05 ± 28.37	161.98 ± 22.99	243.02 ± 67.87	238.14 ± 48.97	0.99 ± 0.14	1.35 ± 0.54	1.000	0.690
11	Serine	156.87 ± 271.98	265.26 ± 229.40	972.71 ± 409.36	155.49 ± 42.21	1.69 ± 1.46	0.98 ± 0.20	0.222	0.008
12	Threonine	1103.15 ± 721.20	1479.07 ± 356.14	265.74 ± 45.09	242.98 ± 45.46	1.34 ± 0.32	0.16 ± 0.04	0.421	0.421
13	γ-Aminobutyric acid	164.54 ± 37.76	155.40 ± 14.05	21.12 ± 6.09	17.27 ± 3.18	0.94 ± 0.09	0.91 ± 0.17	0.310	0.151
14	Phenylalanine	228.55 ± 28.39	251.92 ± 18.32	794.89 ± 230.34	863.13 ± 161.21	1.10 ± 0.08	1.09 ± 0.20	0.310	0.690
15	Cysteine	48.87 ± 28.84	51.20 ± 20.87	861.29 ± 128.55	772.81 ± 69.17	1.05 ± 0.43	0.90 ± 0.08	0.548	0.222
16	Aspartic acid	330.83 ± 150.89	358.01 ± 79.24	2462.76 ± 769.07	1158.08 ± 219.74	1.08 ± 0.24	0.47 ± 0.09	0.690	0.095
17	4-Hydroxyproline	33.36 ± 10.10	23.66 ± 16.25	3.15 ± 0.16	2.73 ± 0.22	0.71 ± 0.49	0.87 ± 0.07	0.151	0.032
18	Glutamic_acid	1795.35 ± 834.52	1904.38 ± 422.69	4197.56 ± 1357.95	2031.22 ± 401.71	1.06 ± 0.24	0.48 ± 0.10	0.841	0.056
19	Asparagine	46.10 ± 46.67	56.90 ± 36.48	N.D.[a]	N.D.[a]	1.23 ± 0.79	-	0.421	-
20	Ornithine	61.72 ± 18.83	87.05 ± 13.25	433.28 ± 157.33	696.15 ± 266.92	1.41 ± 0.21	1.61 ± 0.62	0.032	0.095
21	α-Aminoadipic acid	7.12 ± 5.62	6.71 ± 8.46	6.20 ± 1.19	7.62 ± 2.35	0.94 ± 1.19	1.23 ± 0.38	0.690	0.310
22	Glutamine	848.84 ± 280.73	1091.51 ± 304.31	2654.83 ± 877.57	1734.77 ± 343.57	1.29 ± 0.36	0.65 ± 0.13	0.222	0.151
23	Lysine	546.75 ± 105.99	680.29 ± 84.73	1551.78 ± 480.97	1292.32 ± 154.37	1.24 ± 0.15	0.83 ± 0.10	0.095	0.151
24	Histidine	440.57 ± 125.58	610.18 ± 239.30	1750.86 ± 684.24	2143.87 ± 831.95	1.38 ± 0.54	1.22 ± 0.48	0.222	0.548
25	Tyrosine	409.69 ± 63.86	665.84 ± 151.03	76.68 ± 32.90	102.74 ± 34.92	1.63 ± 0.37	1.34 ± 0.46	0.032	0.310
26	Tryptophan	53.16 ± 67.11	102.46 ± 66.25	3373.07 ± 1733.98	751.65 ± 265.63	1.93 ± 1.25	0.22 ± 0.08	0.151	0.095
27	N-methyl-aspartic_acid	N.D.[a]	N.D.[a]	3243.88 ± 4.98	3228.26 ± 37.79	-	1.00 ± 0.01	-	0.841
28	β-Aminoisobutyric acid	N.D.[a]	N.D.[a]	N.D.[a]	N.D.[a]	-	-	-	-
29	Homocysteine	N.D.[a]	N.D.[a]	N.D.[a]	N.D.[a]	-	-	-	-
30	Pyruvic acid	9.98 ± 6.92	7.08 ± 3.12	35.16 ± 5.07	40.08 ± 2.30	0.71 ± 0.31	1.14 ± 0.07	0.548	0.095
31	Acetoacetic acid	22.42 ± 9.42	22.81 ± 4.67	N.D.[a]	N.D.[a]	1.02 ± 0.21	-	0.690	-
32	Lactic acid	360.98 ± 52.86	309.80 ± 36.79	239.02 ± 28.32	250.30 ± 25.19	0.86 ± 0.10	1.05 ± 0.11	0.222	0.548
33	Glycolic acid	40.02 ± 4.87	39.05 ± 2.79	41.81 ± 5.11	47.31 ± 4.78	0.98 ± 0.07	1.13 ± 0.11	1.000	0.222
34	2-Hydroxybutyric acid	0.36 ± 0.02	0.79 ± 0.08	N.D.[a]	N.D.[a]	2.22 ± 0.21	-	0.008	-
35	3-Hydroxybutyric acid	5.42 ± 1.81	6.68 ± 2.29	1.78 ± 0.87	6.43 ± 3.95	1.23 ± 0.42	3.60 ± 2.21	0.548	0.032

Table 1. Continued.

No.	Metabolite	Amount (ng/mg, mean ± SD)				Normalized value (mean ± SD)[b]		*p*-value[c]	
		Kidney		Spleen					
		Control	Sepsis	Control	Sepsis	Kidney	Spleen	Kidney	Spleen
36	Malonic acid	2.25 ± 0.19	2.54 ± 0.22	1.03 ± 0.16	1.24 ± 0.24	1.13 ± 0.10	1.21 ± 0.23	0.095	0.151
37	Succinic acid	316.26 ± 15.85	346.77 ± 30.55	22.51 ± 7.70	28.08 ± 5.23	1.10 ± 0.10	1.25 ± 0.23	0.056	0.095
38	Fumaric acid	3.59 ± 0.48	3.83 ± 1.75	7.10 ± 0.59	8.68 ± 1.38	1.07 ± 0.49	1.22 ± 0.19	0.548	0.095
39	Oxaloacetic acid	4.08 ± 0.51	4.37 ± 0.41	3.38 ± 0.30	3.53 ± 0.15	1.07 ± 0.10	1.05 ± 0.04	0.310	0.690
40	α-Ketoglutaric acid	2.91 ± 0.12	2.98 ± 0.12	2.88 ± 0.19	3.44 ± 0.70	1.02 ± 0.04	1.19 ± 0.24	0.310	0.056
41	4-Hydroxyphenylacetic acid	0.22 ± 0.01	0.26 ± 0.05	0.50 ± 0.01	0.50 ± 0.01	1.17 ± 0.25	1.01 ± 0.02	0.056	0.421
42	Malic acid	22.61 ± 2.87	34.86 ± 8.26	59.17 ± 9.04	69.15 ± 8.92	1.54 ± 0.37	1.17 ± 0.15	0.016	0.222
43	2-Hydroxyglutaric acid	5.02 ± 0.11	4.99 ± 0.31	N.D.[a]	N.D.[a]	0.99 ± 0.06	-	0.690	-
44	*cis*-Aconitic acid	3.61 ± 0.12	4.15 ± 0.48	1.33 ± 0.22	1.59 ± 0.10	1.15 ± 0.13	1.19 ± 0.08	0.016	0.032
45	4-Hydroxyphenyllactic acid	N.D.[a]	N.D.[a]	0.70 ± 0.02	0.81 ± 0.04	-	1.15 ± 0.05	-	0.008
46	Citric acid	N.D.[a]	N.D.[a]	20.02 ± 6.00	24.09 ± 3.10	-	1.20 ± 0.15	-	0.310
47	Myristic acid	2.02 ± 0.31	2.83 ± 0.91	N.D.[a]	N.D.[a]	1.05 ± 0.79	-	1.000	-
48	Palmitoleic acid	4.01 ± 0.55	7.67 ± 3.56	1.13 ± 0.32	2.91 ± 0.26	1.91 ± 0.89	2.59 ± 0.23	0.690	0.008
49	Palmitic acid	97.93 ± 17.12	95.88 ± 37.23	19.00 ± 12.60	46.48 ± 22.76	0.98 ± 0.38	2.45 ± 1.20	0.690	0.056
50	Linoleic acid	116.55 ± 13.31	130.41 ± 63.33	19.25 ± 5.61	38.41 ± 6.48	1.12 ± 0.54	2.00 ± 0.34	0.690	0.008
51	Oleic acid	62.05 ± 6.86	91.70 ± 38.85	11.11 ± 2.53	27.50 ± 5.31	1.48 ± 0.63	2.48 ± 0.48	0.690	0.012
52	a-Linolenic acid	1.75 ± 0.27	2.21 ± 0.41	N.D.[a]	N.D.[a]	0.95 ± 0.66	-	1.000	-
53	Stearic acid	60.56 ± 13.47	54.56 ± 18.65	19.55 ± 21.19	21.97 ± 23.85	0.90 ± 0.31	1.12 ± 1.22	0.310	0.091
54	Arachidonic acid	143.81 ± 17.60	91.61 ± 56.80	58.86 ± 8.36	69.90 ± 12.33	0.64 ± 0.39	1.19 ± 0.21	0.095	0.151
55	Gondoic acid	1.79 ± 0.14	2.71 ± 0.84	0.37 ± 0.12	0.63 ± 0.16	1.52 ± 0.47	1.70 ± 0.44	0.421	0.056
56	Eicosadienoic acid	7.33 ± 0.89	6.15 ± 2.64	2.95 ± 0.97	5.40 ± 1.15	0.84 ± 0.36	1.83 ± 0.39	0.421	0.008
57	Arachidic acid	0.86 ± 0.20	1.12 ± 0.31	N.D.[a]	N.D.[a]	1.31 ± 0.36	-	0.690	-
58	Docosahexaenoic acid	35.46 ± 4.44	30.57 ± 8.68	N.D.[a]	N.D.[a]	0.65 ± 0.48	-	0.142	-
59	Adrenic acid	41.29 ± 5.17	50.60 ± 7.14	71.32 ± 18.70	104.91 ± 20.82	0.92 ± 0.63	1.47 ± 0.29	1.000	0.056
60	Behenic acid	0.87 ± 0.08	0.94 ± 0.17	1.09 ± 0.35	N.D.[a]	1.08 ± 0.19	-	0.526	0.007
61	Nervonic acid	0.65 ± 0.03	0.71 ± 0.08	1.18 ± 0.26	0.83 ± 0.09	1.08 ± 0.12	0.70 ± 0.07	0.548	0.016
62	Lignoceric acid	3.32 ± 0.71	3.27 ± 0.21	2.87 ± 0.38	N.D.[a]	0.98 ± 0.06	-	0.841	-
63	Cerotic acid	N.D.[a]	N.D.[a]	3.16 ± 0.98	1.41 ± 0.23	-	0.45 ± 0.07	-	0.008
64	5,6-Dihydrouridine	0.015 ± 0.00081	0.018 ± 0.0026	0.022 ± 0.0043	0.028 ± 0.0020	1.63 ± 0.30	1.23 ± 0.09	0.095	0.095
65	Pseudouridine	0.036 ± 0.0038	0.06 ± 0.01	0.08 ± 0.01	0.08 ± 0.01	1.14 ± 0.04	0.98 ± 0.10	0.016	0.690
66	Cytidine	0.019 ± 0.00094	0.021 ± 0.00066	1.20 ± 0.13	1.08 ± 0.13	0.83 ± 0.13	0.89 ± 0.11	0.008	0.222
67	Uridine	0.30 ± 0.03	0.24 ± 0.04	1.17 ± 0.18	0.65 ± 0.13	0.92 ± 0.13	0.55 ± 0.11	0.056	0.008
68	Inosine	1.09 ± 0.07	1.00 ± 0.14	1.28 ± 0.17	1.16 ± 0.15	1.07 ± 0.08	0.90 ± 0.12	0.222	0.222
69	Guanosine	0.11 ± 0.01	0.12 ± 0.01	0.58 ± 0.08	0.45 ± 0.09	1.29 ± 0.14	0.79 ± 0.16	0.310	0.095
70	Xanthosine	0.042 ± 0.0030	0.05 ± 0.01	0.08 ± 0.01	0.13 ± 0.03	1.42 ± 0.20	1.57 ± 0.32	0.016	0.008

Table 1. Continued.

No.	Metabolite	Amount (ng/mg, mean ± SD)				Normalized value (mean ± SD)[b]		*p*-value[c]	
		Kidney		Spleen					
		Control	Sepsis	Control	Sepsis	Kidney	Spleen	Kidney	Spleen
71	1-Methylguanosine	0.0046 ± 0.00032	0.0065 ± 0.00090	0.014 ± 0.0012	0.014 ± 0.0015	1.10 ± 0.08	0.95 ± 0.11	0.008	0.548
72	N^2-Methylguanosine	0.012 ± 0.0011	0.014 ± 0.00097	0.033 ± 0.0047	0.031 ± 0.0042	0.90 ± 0.08	0.94 ± 0.13	0.095	0.421
73	Adenosine	0.10 ± 0.01	0.09 ± 0.01	0.05 ± 0.01	0.03 ± 0.01	1.08 ± 0.08	0.60 ± 0.16	0.421	0.032
74	N^2,N^2-Dimethylguanosine	0.0050 ± 0.00039	0.0053 ± 0.00039	0.011 ± 0.0011	0.012 ± 0.0016	1.28 ± 0.29	1.05 ± 0.14	0.151	0.690
75	5′-Deoxy-5′methylthioadenosine	0.03 ± 0.01	0.04 ± 0.01	0.55 ± 0.08	0.97 ± 0.38	1.63 ± 0.30	1.76 ± 0.69	0.421	0.151
76	5-Methylcytidine	N.D.[a]	N.D.[a]	0.012 ± 0.0019	0.015 ± 0.0025	-	1.17 ± 0.20	-	0.151
77	Picolinic acid	0.51 ± 0.06	0.56 ± 0.13	0.21 ± 0.04	0.16 ± 0.03	1.10 ± 0.24	0.74 ± 0.16	0.690	0.056
78	5-Hydroxytryptophan	0.05 ± 0.01	0.10 ± 0.07	N.D.[a]	N.D.[a]	1.91 ± 1.31	-	0.016	-
79	Kynurenine	0.18 ± 0.02	0.72 ± 1.16	0.25 ± 0.02	0.25 ± 0.01	4.07 ± 6.54	0.99 ± 0.06	0.095	1.000
80	Xanthurenic acid	0.40 ± 0.06	0.47 ± 0.12	0.77 ± 0.12	0.84 ± 0.13	1.18 ± 0.31	1.10 ± 0.16	0.310	0.310
81	Kynurenic acid	0.01 ± 0.01	0.04 ± 0.01	N.D.[a]	N.D.[a]	4.08 ± 1.28	-	0.008	-
82	Epinephrine	0.0046 ± 0.00084	0.018 ± 0.0044	0.18 ± 0.03	0.13 ± 0.04	3.91 ± 0.95	0.73 ± 0.21	0.008	0.056
83	Normetanephrine	0.12 ± 0.04	0.13 ± 0.04	0.25 ± 0.07	0.15 ± 0.06	0.13 ± 0.04	0.60 ± 0.23	1.000	0.032
84	DOPA	0.10 ± 0.02	0.22 ± 0.19	0.20 ± 0.03	0.12 ± 0.05	0.22 ± 0.19	0.63 ± 0.27	0.548	0.056
85	Serotonin	N.D.[a]	N.D.[a]	0.03 ± 0.02	0.03 ± 0.01	-	0.87 ± 0.39	-	1.000
86	Anthranilic acid	N.D.[a]	N.D.[a]	N.D.[a]	N.D.[a]	-	-	-	-

[a] N.D., Not determined.

[b] Values normalized to the corresponding control mean values and SD, standard deviation.

[c] Mann–Whitney U test.

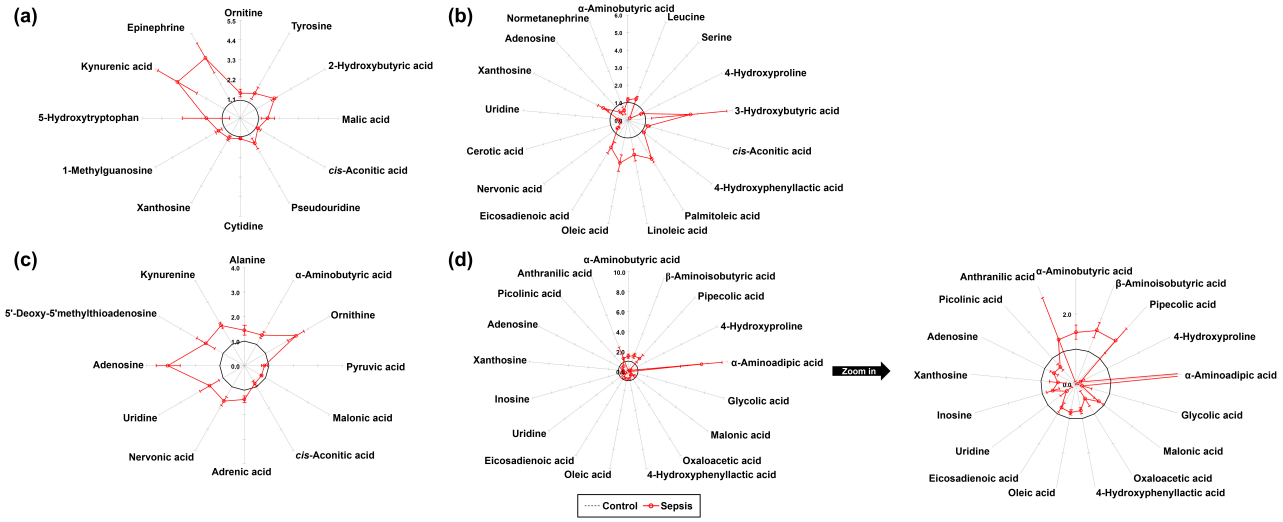

Fig. 2. Star symbol plot of significant metabolites in tissues from control and sepsis mice. (a) Kidney (12 metabolites), (b) Spleen (17 metabolites), (c) Lung (12 metabolites), and (d) Liver (17 metabolites).

3. Results

3.1 Metabolomic Profiling of Kidney Tissue

In total, 77 metabolites were identified in the kidney tissues of both control and sepsis groups, including 26 AAs, 15 OAs, 16 FAs, 12 NSs, and 8 KP metabolites. Quantitative differences in the metabolite profiles between the two groups are presented in Table 1. Normalized values of individual metabolites were visualized using star plots, enabling a clear observation of sepsis-induced metabolic alterations (Table 1, **Supplementary Fig. 1**). Compared to the control group, the sepsis group exhibited significant increases in the levels of ornithine (p = 0.032), tyrosine (p = 0.032), 2-hydroxybutyric acid (p = 0.008), malic acid (p = 0.016), *cis*-aconitic acid (p = 0.016), pseudouridine (p = 0.016), cytidine (p = 0.008), xanthosine (p = 0.016), 1-methylguanosine (p = 0.008), 5-hydroxytryptophan (p = 0.016), kynurenic acid (p = 0.008), and epinephrine (p = 0.008), as determined using the Mann–Whitney U test (Table 1, Fig. 2a).

3.2 Metabolomic Profiling of Spleen Tissue

A total of 72 metabolites were identified in the spleen tissues of both the control and sepsis groups, comprising 25 AAs, 14 OAs, 13 FAs, 13 NSs, and 7 KP metabolites. A quantitative comparison of the metabolite profiles between the two groups is presented in Table 1. Normalized values for each metabolite were visualized using star plots, which enabled intuitive monitoring of sepsis-induced metabolic alterations (Table 1, **Supplementary Fig. 2**). The sepsis group showed significantly higher levels of several metabolites in spleen tissue than the control group, as determined using the Mann–Whitney U test. These metaboltes included α-aminobutyric acid (p = 0.016), leucine (p = 0.032), 3-hydroxybutyric acid (p = 0.032), *cis*-aconitic acid (p = 0.032), 4-hydroxyphenyllactic acid (p = 0.008), palmitoleic acid (p = 0.008), linoleic acid (p = 0.008), oleic acid (p = 0.012), eicosadienoic acid (p = 0.008), and xanthosine (p = 0.008). In contrast, significant decreases were observed in the levels of serine (p = 0.008), 4-hydroxyproline (p = 0.032), nervonic acid (p = 0.016), cerotic acid (p = 0.008), uridine (p = 0.008), adenosine (p = 0.032), and normetanephrine (p = 0.032) (Table 1, Fig. 2b).

3.3 Metabolomic Profiling of Lung Tissue

A total of 70 metabolites were identified in the lung tissues of both the control and sepsis groups, including 24 AAs, 15 OAs, 14 FAs, 12 NSs, and 5 KPs. Quantitative comparisons of the metabolite profiles between the two groups are presented in Table 2. Normalized metabolite levels were visualized using star plots, which enabled intuitive monitoring of sepsis-associated metabolic alterations (Table 2, **Supplementary Fig. 3**). According to the Mann–Whitney U test, several metabolites in the lung tissue showed significant alterations in the sepsis group compared to those in the control group. Notably, alanine (p = 0.008), α-aminoadipic acid (p = 0.008), ornithine (p = 0.008), uridine (p = 0.032), adenosine (p = 0.032), MTA (p = 0.032), and kynurenine (p = 0.008) levels significantly increased in the sepsis group (Table 1). In contrast, significant decreases were observed in lactic acid (p = 0.032), succinic acid (p = 0.016), *cis*-aconitic acid (p = 0.032), eicosadienoic acid (p = 0.016), and adrenic acid (p = 0.016) in the sepsis group (Table 2, Fig. 2c).

3.4 Metabolomic Profiling of Liver Tissue

A total of 78 metabolites were identified in the liver tissues of both the control and sepsis groups, including 28 AAs, 16 OAs, 13 FAs, 12 NSs, and 9 KPs. Quantitative comparisons of the metabolite profiles between the two gr-

Table 2. Levels of amino acid, organic acid, fatty acid, nucleoside, and kynurenine pathway metabolite in lung and liver tissues from the control and sepsis groups.

No.	Metabolite	Amount (ng/mg, mean ± SD)				Normalized value (mean ± SD)[b]		*p*-value[c]	
		Lung		Liver					
		Control	Sepsis	Control	Sepsis	Lung	Liver	Lung	Liver
1	Alanine	132.73 ± 16.92	191.32 ± 25.53	914.25 ± 163.15	979.10 ± 248.44	1.44 ± 0.19	1.07 ± 0.27	0.008	1.000
2	Glycine	323.42 ± 129.31	679.33 ± 239.15	375.57 ± 149.15	594.02 ± 172.25	2.10 ± 0.74	1.58 ± 0.46	0.056	0.095
3	α-Aminobutyric acid	0.58 ± 0.05	0.83 ± 0.09	3.31 ± 0.73	4.91 ± 0.66	1.44 ± 0.15	1.48 ± 0.20	0.008	0.008
4	Valine	45.31 ± 6.73	44.12 ± 9.73	257.84 ± 50.44	302.86 ± 95.48	0.97 ± 0.21	1.17 ± 0.37	0.841	0.222
5	Leucine	166.85 ± 21.07	180.66 ± 31.99	405.80 ± 16.12	411.86 ± 41.46	1.08 ± 0.19	1.01 ± 0.10	0.690	0.421
6	Isoleucine	60.68 ± 6.35	65.48 ± 20.96	286.33 ± 114.87	238.59 ± 85.93	1.08 ± 0.35	0.83 ± 0.30	0.548	1.000
7	Proline	37.82 ± 2.35	42.85 ± 11.28	743.74 ± 171.77	640.90 ± 199.11	1.13 ± 0.30	0.86 ± 0.27	0.690	0.310
8	Pipecolic acid	N.D.[a]	N.D.[a]	2.37 ± 0.41	3.99 ± 1.10	-	1.68 ± 0.46	-	0.032
9	Pyroglutamic acid	77.31 ± 11.54	67.10 ± 34.73	580.12 ± 284.74	293.39 ± 271.65	0.87 ± 0.45	0.51 ± 0.47	0.151	0.095
10	Methionine	51.58 ± 9.84	42.09 ± 13.93	142.53 ± 33.37	194.21 ± 88.70	0.82 ± 0.27	1.36 ± 0.62	0.421	0.548
11	Serine	115.74 ± 20.20	122.36 ± 63.79	305.18 ± 372.72	164.72 ± 72.83	1.06 ± 0.55	0.54 ± 0.24	0.841	1.000
12	Threonine	87.45 ± 9.59	99.93 ± 24.59	1029.27 ± 1298.50	309.03 ± 168.65	1.14 ± 0.28	0.30 ± 0.16	0.421	0.151
13	γ-Aminobutyric acid	5.82 ± 1.96	6.15 ± 1.48	70.74 ± 8.03	73.30 ± 23.13	1.06 ± 0.25	1.04 ± 0.33	1.000	0.690
14	Phenylalanine	100.67 ± 19.65	113.45 ± 27.96	401.45 ± 58.54	497.41 ± 185.49	1.13 ± 0.28	1.24 ± 0.46	0.310	0.222
15	Cysteine	253.68 ± 24.44	280.91 ± 23.94	12.00 ± 6.76	26.48 ± 14.23	1.11 ± 0.09	2.21 ± 1.19	0.151	0.222
16	Aspartic acid	233.89 ± 29.09	277.53 ± 58.41	373.52 ± 70.18	471.90 ± 103.23	1.19 ± 0.25	1.26 ± 0.28	0.310	0.095
17	4-Hydroxyproline	2.62 ± 0.41	1.94 ± 0.78	24.03 ± 30.00	3.53 ± 2.76	0.74 ± 0.30	0.15 ± 0.12	0.151	0.032
18	Glutamic_acid	373.17 ± 45.09	400.34 ± 79.01	1464.92 ± 259.71	1819.71 ± 441.53	1.07 ± 0.21	1.24 ± 0.30	0.421	0.151
19	Asparagine	N.D.[a]	N.D.[a]	70.72 ± 11.73	81.01 ± 47.68	-	1.15 ± 0.67	-	1.000
20	Ornithine	26.12 ± 16.08	63.58 ± 9.93	76.70 ± 20.58	188.04 ± 105.84	2.43 ± 0.38	2.45 ± 1.38	0.008	0.222
21	α-Aminoadipic acid	3.55 ± 1.62	3.80 ± 1.35	5.32 ± 2.23	39.40 ± 11.22	1.07 ± 0.38	7.41 ± 2.11	0.548	0.008
22	Glutamine	429.11 ± 99.46	520.18 ± 154.05	1925.50 ± 426.46	1514.16 ± 564.56	1.21 ± 0.36	0.79 ± 0.29	0.548	0.222
23	Lysine	196.41 ± 19.12	204.80 ± 9.95	210.47 ± 59.70	366.24 ± 198.20	1.04 ± 0.05	1.74 ± 0.94	0.222	0.421
24	Histidine	144.23 ± 20.06	185.13 ± 37.63	948.99 ± 248.71	1008.74 ± 220.11	1.28 ± 0.26	1.06 ± 0.23	0.151	0.548
25	Tyrosine	16.62 ± 7.01	11.51 ± 7.31	868.17 ± 199.54	1621.03 ± 858.84	0.69 ± 0.44	1.87 ± 0.99	0.095	0.222
26	Tryptophan	N.D.[a]	N.D.[a]	14.45 ± 5.13	51.02 ± 42.11	-	3.53 ± 2.91	-	0.548
27	N-methyl-aspartic_acid	1596.45 ± 6.91	1591.55 ± 13.01	N.D.[a]	N.D.[a]	1.00 ± 0.01	-	0.548	-
28	β-Aminoisobutyric acid	N.D.[a]	N.D.[a]	1.54 ± 0.33	2.54 ± 0.35	-	1.65 ± 0.23	-	0.008
29	Homocysteine	N.D.[a]	N.D.[a]	24.03 ± 30.00	3.53 ± 2.76	-	1.15 ± 0.54	-	0.690
30	Pyruvic acid	27.36 ± 4.65	24.18 ± 5.38	34.04 ± 31.29	13.85 ± 7.20	0.88 ± 0.20	0.70 ± 0.51	0.548	0.421
31	Acetoacetic acid	N.D.[a]	N.D.[a]	261.04 ± 207.65	143.80 ± 66.73	-	0.41 ± 0.21	-	0.690
32	Lactic acid	2758.08 ± 295.24	2255.58 ± 342.36	630.12 ± 413.53	193.51 ± 170.82	0.82 ± 0.12	0.55 ± 0.26	0.032	0.095
33	Glycolic acid	39.24 ± 3.31	35.50 ± 3.15	418.06 ± 235.66	75.33 ± 113.43	0.90 ± 0.08	0.31 ± 0.27	0.151	0.032
34	2-Hydroxybutyric acid	N.D.[a]	N.D.[a]	3.25 ± 1.97	2.91 ± 0.44	-	0.18 ± 0.27	-	0.690
35	3-Hydroxybutyric acid	2.90 ± 1.43	4.96 ± 4.02	17.63 ± 14.72	12.36 ± 9.01	1.71 ± 1.39	0.90 ± 0.13	0.548	0.841

Table 2. Continued.

No.	Metabolite	Amount (ng/mg, mean ± SD)				Normalized value (mean ± SD)[b]		*p*-value[c]	
		Lung		Liver					
		Control	Sepsis	Control	Sepsis	Lung	Liver	Lung	Liver
36	Malonic acid	1.07 ± 0.16	1.10 ± 0.34	2.90 ± 0.14	2.37 ± 0.46	1.03 ± 0.31	0.82 ± 0.16	0.841	0.016
37	Succinic acid	3.44 ± 0.74	2.77 ± 0.15	548.38 ± 109.82	629.37 ± 123.58	0.81 ± 0.04	1.15 ± 0.23	0.016	0.548
38	Fumaric acid	5.67 ± 0.67	7.04 ± 1.60	6.69 ± 1.18	6.28 ± 1.35	1.24 ± 0.28	0.94 ± 0.20	0.151	0.841
39	Oxaloacetic acid	1.27 ± 0.19	1.17 ± 0.10	9.67 ± 1.58	4.69 ± 2.44	0.92 ± 0.08	0.49 ± 0.25	0.222	0.032
40	α-Ketoglutaric acid	1.95 ± 0.26	1.71 ± 0.06	7.90 ± 0.90	5.46 ± 2.08	0.88 ± 0.03	0.69 ± 0.26	0.222	0.095
41	4-Hydroxyphenylacetic acid	0.56 ± 0.01	0.56 ± 0.01	0.26 ± 0.01	0.28 ± 0.03	1.00 ± 0.01	1.10 ± 0.11	0.841	0.151
42	Malic acid	39.26 ± 5.17	46.72 ± 12.30	36.10 ± 11.82	56.35 ± 31.91	1.19 ± 0.31	1.56 ± 0.88	0.548	0.310
43	2-Hydroxyglutaric acid	3.31 ± 0.47	3.61 ± 0.48	10.86 ± 2.25	6.93 ± 3.73	1.09 ± 0.15	0.64 ± 0.34	0.222	0.151
44	*cis*-Aconitic acid	0.78 ± 0.07	0.66 ± 0.09	3.48 ± 0.01	3.52 ± 0.06	0.84 ± 0.11	1.01 ± 0.02	0.032	0.151
45	4-Hydroxyphenyllactic acid	0.93 ± 0.02	0.95 ± 0.03	0.46 ± 0.05	0.36 ± 0.04	1.03 ± 0.03	0.77 ± 0.10	0.222	0.032
46	Citric acid	12.15 ± 3.68	14.32 ± 1.50	N.D.[a]	N.D.[a]	1.18 ± 0.12	-	0.548	-
47	Myristic acid	2.60 ± 0.41	2.24 ± 0.47	1.35 ± 0.57	1.65 ± 1.02	0.86 ± 0.18	1.23 ± 0.76	0.222	0.690
48	Palmitoleic acid	6.04 ± 1.70	7.99 ± 1.48	7.73 ± 1.78	6.94 ± 0.79	1.32 ± 0.24	0.90 ± 0.10	0.095	0.310
49	Palmitic acid	89.70 ± 28.76	110.95 ± 7.65	185.45 ± 41.85	163.86 ± 20.63	1.24 ± 0.09	0.88 ± 0.11	0.151	0.222
50	Linoleic acid	50.65 ± 9.88	53.97 ± 1.61	186.83 ± 35.39	159.88 ± 45.46	1.07 ± 0.03	0.86 ± 0.24	0.841	0.421
51	Oleic acid	61.03 ± 17.05	74.17 ± 7.38	108.93 ± 16.69	89.33 ± 7.68	1.22 ± 0.12	0.82 ± 0.07	0.151	0.032
52	a-Linolenic acid	N.D.[a]	N.D.[a]	2.02 ± 0.42	1.73 ± 0.34	-	0.86 ± 0.17	-	0.151
53	Stearic acid	26.76 ± 11.13	33.49 ± 3.50	73.06 ± 19.05	71.46 ± 10.10	1.25 ± 0.13	0.98 ± 0.14	0.222	0.421
54	Arachidonic acid	52.84 ± 10.17	64.75 ± 13.25	151.64 ± 42.15	106.26 ± 47.60	1.23 ± 0.25	0.70 ± 0.31	0.095	0.095
55	Gondoic acid	1.36 ± 0.51	1.82 ± 0.32	1.45 ± 0.35	1.26 ± 0.16	1.34 ± 0.23	0.86 ± 0.11	0.151	0.310
56	Eicosadienoic acid	3.36 ± 0.91	4.64 ± 0.45	5.70 ± 0.79	4.47 ± 0.93	1.38 ± 0.13	0.78 ± 0.16	0.016	0.032
57	Arachidic acid	0.67 ± 0.13	0.63 ± 0.05	N.D.[a]	N.D.[a]	0.93 ± 0.07	-	0.841	-
58	Docosahexaenoic acid	N.D.[a]	N.D.[a]	29.16 ± 5.51	29.11 ± 7.21	-	1.00 ± 0.25	-	1.000
59	Adrenic acid	111.70 ± 40.15	186.49 ± 22.70	47.71 ± 22.64	42.67 ± 17.46	1.67 ± 0.20	0.89 ± 0.37	0.016	0.548
60	Behenic acid	0.95 ± 0.05	0.95 ± 0.08	N.D.[a]	N.D.[a]	1.00 ± 0.08	-	0.402	-
61	Nervonic acid	1.00 ± 0.22	1.20 ± 0.06	0.76 ± 0.16	0.62 ± 0.05	1.20 ± 0.06	0.81 ± 0.06	0.095	0.151
62	Lignoceric acid	3.55 ± 0.73	3.17 ± 0.02	N.D.[a]	N.D.[a]	0.89 ± 0.01	-	0.690	-
63	Cerotic acid	N.D.[a]	N.D.[a]	N.D.[a]	N.D.[a]	-	-	-	-
64	5,6-Dihydrouridine	0.0037 ± 0.00041	0.0056 ± 0.0016	0.0041 ± 0.00025	0.010 ± 0.0044	1.50 ± 0.43	1.01 ± 0.30	0.095	0.151
65	Pseudouridine	0.0071 ± 0.0016	0.01 ± 0.01	0.07 ± 0.01	0.07 ± 0.02	1.94 ± 0.74	1.41 ± 0.82	0.151	0.310
66	Cytidine	0.22 ± 0.02	0.20 ± 0.02	0.041 ± 0.00060	0.06 ± 0.03	0.91 ± 0.09	0.33 ± 0.22	0.310	0.690
67	Uridine	0.09 ± 0.02	0.15 ± 0.04	0.98 ± 0.14	0.32 ± 0.22	1.63 ± 0.45	0.69 ± 0.19	0.032	0.008
68	Inosine	0.53 ± 0.04	0.61 ± 0.16	1.70 ± 0.14	1.17 ± 0.32	1.15 ± 0.30	1.55 ± 0.79	1.000	0.016
69	Guanosine	0.13 ± 0.02	0.19 ± 0.05	0.18 ± 0.02	0.28 ± 0.14	1.41 ± 0.41	0.52 ± 0.25	0.151	0.151
70	Xanthosine	0.012 ± 0.0026	0.010 ± 0.0022	0.48 ± 0.03	0.25 ± 0.12	0.84 ± 0.18	1.43 ± 0.56	0.222	0.016

Table 2. Continued.

No.	Metabolite	Amount (ng/mg, mean ± SD)				Normalized value (mean ± SD)[b]		*p*-value[c]	
		Lung		Liver					
		Control	Sepsis	Control	Sepsis	Lung	Liver	Lung	Liver
71	1-Methylguanosine	0.0035 ± 0.0013	0.0028 ± 0.00040	0.0032 ± 0.00017	0.0045 ± 0.0018	0.80 ± 0.12	1.35 ± 0.59	0.310	0.151
72	N2-Methylguanosine	0.0040 ± 0.00053	0.0032 ± 0.0012	0.0064 ± 0.00051	0.0086 ± 0.0038	0.80 ± 0.29	0.70 ± 0.11	0.222	0.151
73	Adenosine	0.03 ± 0.03	0.08 ± 0.01	0.35 ± 0.02	0.25 ± 0.04	3.13 ± 0.50	1.30 ± 0.33	0.032	0.008
74	N2,N2-Dimethylguanosine	0.0029 ± 0.00020	0.0027 ± 0.00012	0.0028 ± 0.00011	0.0036 ± 0.00094	0.96 ± 0.04	1.46 ± 0.42	0.222	0.151
75	5′-Deoxy-5′methylthioadenosine	0.24 ± 0.09	0.43 ± 0.10	0.09 ± 0.01	0.13 ± 0.04	1.82 ± 0.42	1.01 ± 0.30	0.032	0.095
76	5-Methylcytidine	N.D.[a]	N.D.[a]	N.D.[a]	N.D.[a]	-	-	-	-
77	Picolinic acid	0.21 ± 0.04	0.14 ± 0.04	0.99 ± 0.41	0.65 ± 0.12	0.67 ± 0.19	0.66 ± 0.12	0.056	0.032
78	5-Hydroxytryptophan	N.D.[a]	N.D.[a]	0.04 ± 0.01	0.05 ± 0.01	-	1.19 ± 0.28	-	0.841
79	Kynurenine	0.20 ± 0.0013	0.37 ± 0.02	0.64 ± 0.27	0.66 ± 0.25	1.89 ± 0.12	1.03 ± 0.38	0.008	1.000
80	Xanthurenic acid	0.13 ± 0.02	0.12 ± 0.01	0.58 ± 0.22	0.60 ± 0.18	0.93 ± 0.10	1.03 ± 0.32	0.690	0.690
81	Kynurenic acid	N.D.[a]	N.D.[a]	0.0069 ± 0.0031	0.0032 ± 0.0012	-	0.46 ± 0.17	-	1.000
82	Epinephrine	0.02 ± 0.01	0.012 ± 0.0039	0.07 ± 0.02	0.04 ± 0.03	0.71 ± 0.23	0.66 ± 0.48	0.222	0.310
83	Normetanephrine	0.13 ± 0.06	0.10 ± 0.05	0.20 ± 0.21	0.12 ± 0.17	0.74 ± 0.43	0.62 ± 0.84	0.548	1.000
84	DOPA	N.D.[a]	N.D.[a]	0.13 ± 0.03	0.08 ± 0.04	-	0.65 ± 0.30	-	0.222
85	Serotonin	N.D.[a]	N.D.[a]	N.D.[a]	N.D.[a]	-	-	-	-
86	Anthranilic acid	N.D.[a]	N.D.[a]	0.01 ± 0.01	0.02 ± 0.01	-	1.36 ± 1.28	-	0.016

[a] N.D., Not determined.

[b] Values normalized to the corresponding control mean values and SD, standard deviation.

[c] Mann–Whitney U test.

oups are presented in Table 2. Normalized values for each metabolite were visualized using star plots, allowing an intuitive assessment of sepsis-induced metabolic alterations (Table 2, **Supplementary Fig. 4**). Based on the Mann–Whitney U test, significant differences in metabolite levels were observed in the liver tissue between the control and sepsis groups. Specifically, the sepsis group exhibited significant increases in α-aminobutyric acid (p = 0.008), pipecolic acid (p = 0.032), α-aminoadipic acid (p = 0.008), β-aminoisobutyric acid (p = 0.008), and anthranilic acid (p = 0.016). In contrast, levels of 4-hydroxyproline (p = 0.032), glycolic acid (p = 0.032), malonic acid (p = 0.016), oxaloacetic acid (p = 0.032), 4-hydroxyphenyllactic acid (p = 0.032), oleic acid (p = 0.032), eicosadienoic acid (p = 0.032), uridine (p = 0.008), inosine (p = 0.016), xanthosine (p = 0.016), adenosine (p = 0.008), and picolinic acid (p = 0.032) were significantly decreased in the sepsis group (Table 2, Fig. 2d).

3.5 Multivariate Statistical Analysis

PCA and PLS-DA were performed for each tissue, and the results are presented in Figs. 3,4. Although the overall metabolic profiles of the control and sepsis groups showed some degree of similarity in the PCA score plot, they were not distinctly separated (Fig. 3). The PCA score plot of kidney, spleen, lung, and liver explained 50.4, 57.7, 58.1, and 68.6% of total variance in PC1 and PC2 (Fig. 3). The corresponding PCA loading scores for all tissues are listed in Table 2. PLS-DA revealed a clear separation between the two groups (Fig. 4). The variable importance in projection (VIP) scores derived from the PLS-DA models are shown in **Supplementary Table 1**.

Metabolites with a VIP score greater than 1.0 were considered to have a strong influence on group separation in PLS-DA. Key metabolites in the kidney included leucine, proline, phenylalanine, 4-hydroxyproline, ornithine, lysine, tyrosine, tryptophan, lactic acid, 2-hydroxybutyric acid, malonic acid, succinic acid, 4-hydroxyphenylacetic acid, malic acid, *cis*-aconitic acid, 5,6-dihydrouridine, pseudouridine, cytidine, uridine, xanthosine, 1-methylguanosine, N^2-methylguanosine, N^2,N^2-dimethylguanosine, 5-hydroxytryptophan, kynurenic acid, and epinephrine (**Supplementary Table 1**). In the spleen, metabolites with VIP $>$1.0 included α-aminobutyric acid, leucine, isoleucine, serine, aspartic acid, 4-hydroxyproline, glutamic acid, tryptophan, 3-hydroxybutyric acid, fumaric acid, *cis*-aconitic acid, 4-hydroxyphenyllactic acid, 5,6-dihydrouridine, uridine, guanosine, xanthosine, adenosine, MTA, picolinic acid, epinephrine, normetanephrine, DOPA, palmitoleic acid, palmitic acid, linoleic acid, oleic acid, stearic acid, gondoic acid, eicosadienoic acid, adrenic acid, behenic acid, nervonic acid, lignoceric acid, and cerotic acid (**Supplementary Table 1**). In the lung, influential metabolites were alanine, glycine, α-aminobutyric acid, cysteine, 4-hydroxyproline, ornithine, histidine, lactic acid, glycolic acid, succinic acid, fumaric acid, α-ketoglutaric acid, *cis*-aconitic acid, 5,6-dihydrouridine, pseudouridine, cytidine, uridine, guanosine, adenosine, MTA, picolinic acid, kynurenine, palmitoleic acid, eicosadienoic acid, adrenic acid, behenic acid, and nervonic acid (**Supplementary Table 1**). In the liver, metabolites contributing significantly to group separation included glycine, α-aminobutyric acid, β-aminoisobutyric acid, pipecolic acid, pyroglutamic acid, aspartic acid, 4-hydroxyproline, ornithine, α-aminoadipic acid, tyrosine, tryptophan, lactic acid, glycolic acid, malonic acid, oxaloacetic acid, α-ketoglutaric acid, 4-hydroxyphenylacetic acid, 2-hydroxyglutaric acid, 4-hydroxyphenyllactic acid, 5,6-dihydrouridine, uridine, inosine, xanthosine, adenosine, N^2,N^2-dimethylguanosine, MTA, picolinic acid, kynurenic acid, epinephrine, DOPA, and arachidonic acid (**Supplementary Table 1**).

3.6 Common Metabolites Among Four Tissues

In the univariate and multivariate analyses, no metabolites were commonly identified across all four tissues (Fig. 5). However, several overlapped between two or three tissues. Cis-aconitic acid was elevated in the kidney and spleen but reduced in the lung, whereas xanthosine increased in the kidney and spleen but decreased in the liver. Uridine and adenosine were upregulated in the lung but downregulated in the spleen and liver. Additionally, eicosadienoic acid was increased in both the spleen and lung but decreased in the liver. In the spleen and liver, α-aminobutyric acid was elevated while 4-hydroxyproline was reduced. In contrast, 4-hydroxyphenyllactic acid increased in the spleen but decreased in the liver.

3.7 Pathway Analysis

Based on the Kyoto Encyclopedia of Genes and Genomes database, potential discriminatory metabolic pathways were identified using a pathway impact value threshold of $\geq$0.1 and a p-value of $<$0.05. In the kidney, significant alterations were observed in tyrosine metabolism; phenylalanine metabolism; and phenylalanine, tyrosine, and tryptophan biosynthesis (Fig. 6a). In the spleen, the significantly altered pathways were arginine biosynthesis; histidine metabolism; tyrosine metabolism; one-carbon pool by folate; linoleic acid metabolism; alanine, aspartate, and glutamate metabolism; cysteine and methionine metabolism; glyoxylate and dicarboxylate metabolism; arginine and proline metabolism; glycine, serine, and threonine metabolism; and glutathione metabolism (Fig. 6b). In the lungs, the significantly altered pathways were one carbon pool by folate; glutathione metabolism; the tricarboxylic acid (TCA) cycle; and alanine, aspartate, and glutamate metabolism (Fig. 6c). In the liver, lysine degradation, glyoxylate and dicarboxylate metabolism, arginine biosynthesis, the one-carbon pool by folate, and the TCA cycle were significantly altered (Fig. 6d).

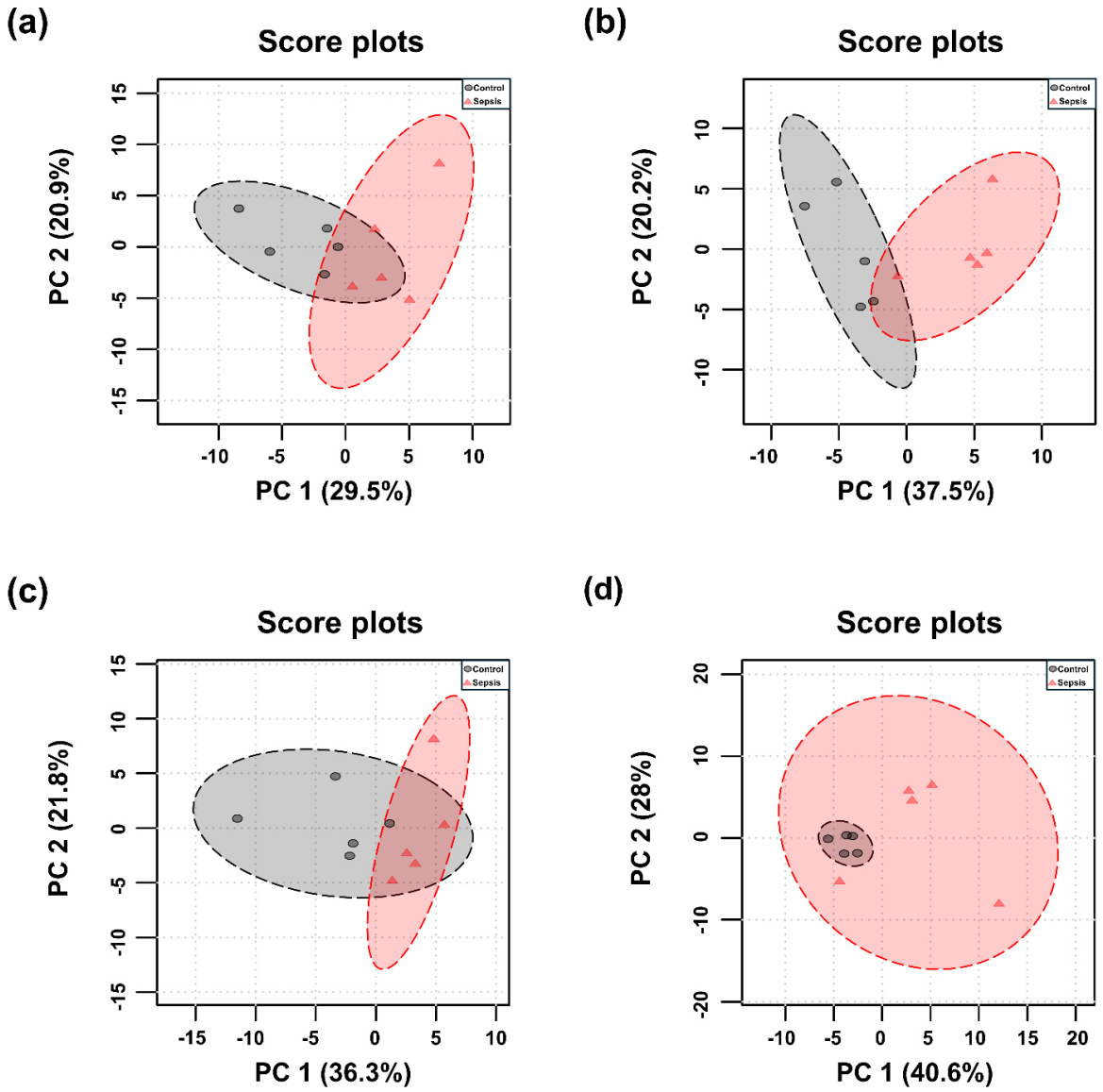

Fig. 3. Principal component analysis (PCA) score plots of metabolites in tissues from control and sepsis mice. PCA score plots the (a) kidney, R^2 = 0.38; *p*-value = 0.005, (b) spleen, R^2 = 0.55; *p*-value = 0.007, (c) lung, R^2 = 0.35; *p*-value = 0.018, and (d) liver R^2 = 0.30; *p*-value = 0.054, based on the profiles of determined metabolites.

4. Discussion

Sepsis is a complex syndrome characterized by considerable clinical heterogeneity, in which organ dysfunction is the primary contributor to morbidity and mortality. The mechanisms underlying organ dysfunction in sepsis possibly involve impaired tissue oxygen delivery; diverse inflammatory responses, including endothelial and microvascular dysfunction; dysregulation of the immune and autonomic nervous systems; and alterations in cellular metabolism [20]. Organ dysfunction resulting from sepsis poses a critical clinical challenge, underscoring the need for biomarkers capable of early diagnosis. Therefore, in this study, we conducted targeted metabolomic analyses of kidney, spleen, lung, and liver tissues to identify potential biomarkers for sepsis and elucidate significantly altered metabolic pathways. For each tissue sample, metabolites showing significant changes in univariate and multivariate analyses were selected, and those involved in sepsis-altered pathways were designated as biomarkers.

In the kidneys, four metabolites (tyrosine, epinephrine, 5-hydroxytryptophan, and kynurenic acid) were identified as potential biomarkers of sepsis-induced injury. The elevated levels of tyrosine observed in the kidney tissue may indicate enhanced activation of inflammatory responses induced by sepsis, as tyrosine serves as a precursor for catecholamines and various intracellular signaling molecules [21]. This accumulation of tyrosine may reflect the progression of renal injury, potentially through its involvement in the regulation of inflammation and activation of cellular signaling pathways. The

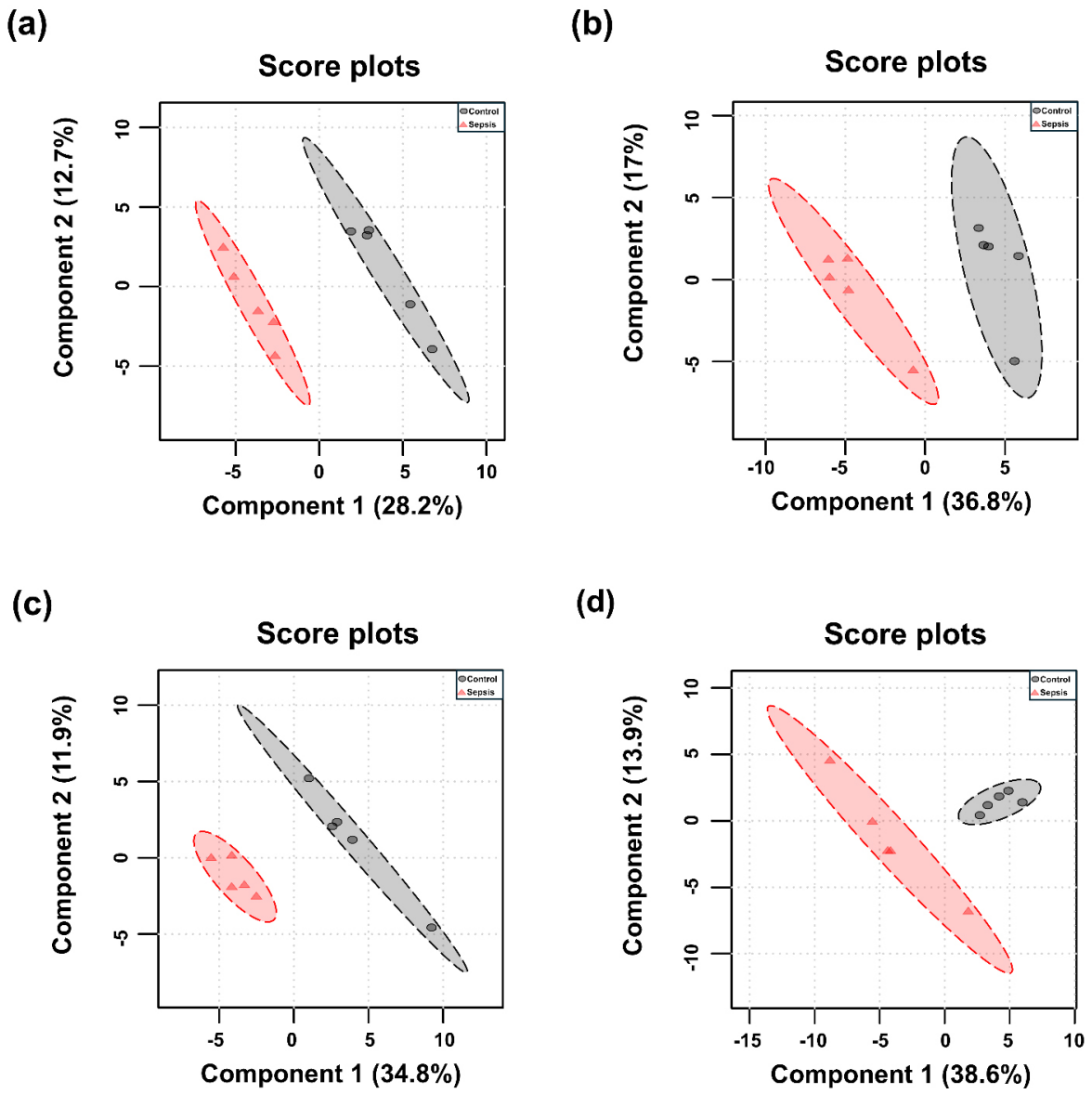

Fig. 4. Partial least squares discriminant analysis (PLS-DA) score plots of determined metabolites in tissues from control and sepsis mice. PLS-DA score plots are shown for the (a) kidney; $R^2 = 0.993$, $Q^2 = 0.727$, (b) spleen; $R^2 = 0.994$, $Q^2 = 0.755$, (c) lung; $R^2 = 0.983$, $Q^2 = 0.609$, and (d) liver; $R^2 = 0.951$, $Q^2 = 0.454$.

kynurenine pathway is the principal route through which the amino acid tryptophan is metabolized; its first step is catalyzed by indoleamine 2,3-dioxygenase (IDO). During sepsis, elevated levels of kynurenine and activation of IDO are reportedly associated with infection-driven immune responses, particularly the release of interferon-γ from monocytes and macrophages [22]. In sepsis, the kidneys may be unable to effectively excrete excessive kynurenic acid. This impaired excretory function may contribute to kynurenine accumulation, indicating disrupted renal handling of kynurenine pathway metabolites during systemic inflammation. In contrast, identified alterations in energy and nucleotide metabolism as key features of SA-AKI, suggesting that methodological differences may reveal distinct pathways within the kidney [11]. Proteomics analysis also revealed interferon regulatory factor 7-related changes in septic AKI [23], indicating that the metabolic disturbances we observed may be linked to upstream protein-level regulation. Moreover, a sequential biopsy study in a porcine model demonstrated early impairments in mitochondrial oxidative phosphorylation and increased uncoupling [24], consistent with our observation that amino acid and catecholamine alterations may reflect mitochondrial dysfunction.

In the spleen, 10 metabolites, including serine, 4-hydroxyproline, normetanephrine, xanthosine, uridine, adenosine, succinic acid, *cis*-aconitic acid, linoleic acid, and eicosadienoic acid, were identified as potential

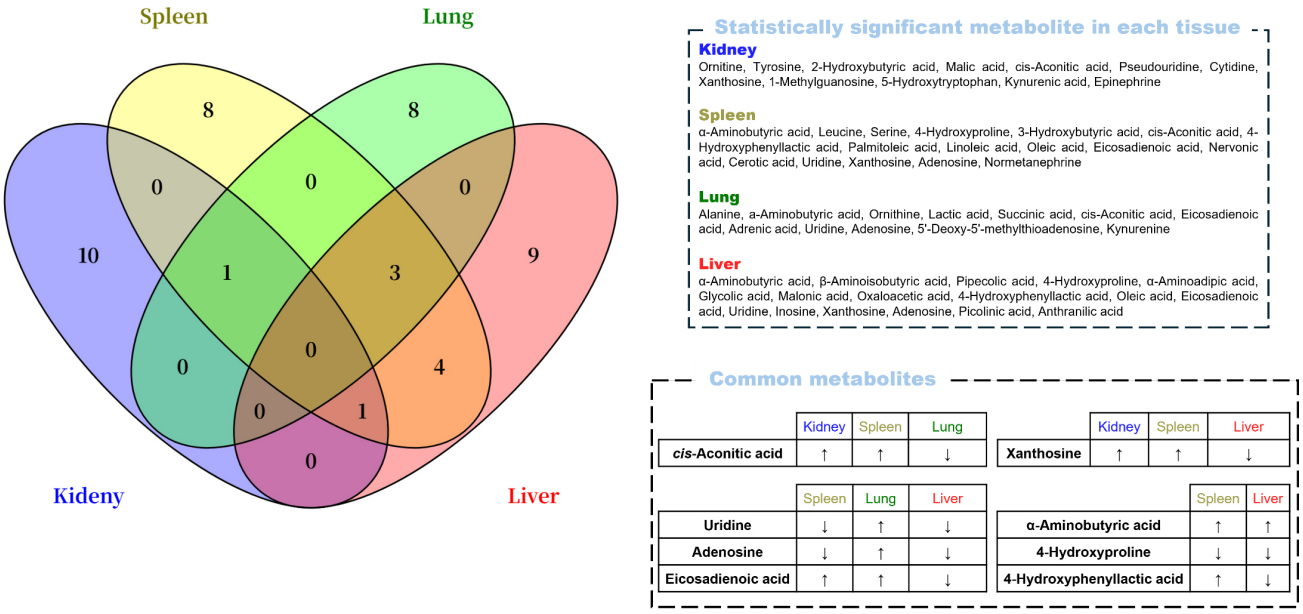

Fig. 5. Venn diagram containing significant metabolites by the univariate and multivariate analyses ($p < 0.05$, VIP score ≥ 1.0) in each tissue. ↑ ; increased in the sepsis group compared with the control group, ↓ ; decreased in the sepsis group compared with the control group.

biomarkers indicative of sepsis-induced tissue injury. Serine is a nonessential amino acid that participates in fatty acid oxidation and muscle metabolism [25]. In sepsis, increased fatty acid oxidation for adenosine triphosphate (ATP) production may lead to serine depletion due to the metabolic demand. In addition, serine has been shown to play a role as an early tissue- and cell type-specific regulator of lipid and mitochondrial metabolic pathways in sepsis [26]. Similarly, 4-hydroxyproline, a marker of collagen breakdown [27], was unexpectedly reduced in septic spleens, likely due to decreased proline availability, limiting its synthesis. Normetanephrine, derived from catecholamine metabolism via catechol-O-methyltransferase, typically reflects sympathetic activity. Although catecholamine levels increase in sepsis [28], normetanephrine levels decrease in the spleen, potentially because of norepinephrine depletion from excessive sympathetic activation [29]. In sepsis, activation of the Xanthine oxidase-ROS axis and enhanced purine catabolism are consistent with the reported elevation of xanthosine under infection- and immune-activated conditions However, the increase in xanthosine itself in sepsis cohorts requires further confirmation [30,31]. Adenosine, a key energy mediator, is generated from ATP degradation and modulates inflammation via A_2A receptors [32,33]. Uridine, the only pyrimidine nucleoside that was significantly altered in the spleen, showed a marked decrease, possibly due to RNA synthesis and immune cell proliferation. Its role in oxidative stress modulation via ferroptosis inhibition and Keap1–Nrf2 signaling is relevant to sepsis pathology [34,35]. The increase in *cis*-aconitic acid levels observed in both the kidney and spleen implied TCA cycle dysfunction and impaired energy production during sepsis. Additionally, early sepsis is associated with enhanced lipolysis and insulin resistance [36–38], driving the use of fatty acids as energy sources. Elevated levels of monounsaturated FAs (palmitoleic and oleic acid), synthesized by Stearoyl-CoA desaturase 1 in the endoplasmic reticulum [39], align with increased lipid mobilization and may support immune activation and membrane remodeling. Similarly, higher levels of omega-6 polyunsaturated FAs and linoleic and eicosadienoic acids suggest enhanced synthesis of pro-inflammatory eicosanoids [40].

In the lung tissue, eight metabolites (alanine, α-aminobutyric acid, ornithine, uridine, adenosine, MTA, succinic acid, and *cis*-aconitic acid) were identified as potential biomarkers reflecting sepsis-induced injury. The enzyme that converts α-aminobutyric acid to α-ketoadipic acid is shared by the kynurenine-to-kynurenic acid conversion step [41], suggesting a potential metabolic link between α-aminobutyric acid accumulation and increased kynurenine activity in sepsis. Ornithine, a key component of the urea cycle, is elevated in septic lungs, possibly because of impaired urea cycle function or reduced amino acid clearance. Additionally, ornithine may be redirected toward polyamine synthesis via ornithine decarboxylase, an enzyme that is upregulated in sepsis and is known to modulate inflammation and support tissue repair [42]. Enhanced kynurenine production in the lungs may also result from inflammation-driven activation of IDO. MTA, an anti-inflammatory metabolite derived from adenosine, was significantly elevated only in the lung tissue. Its accumulation likely reflects increased polyamine biosynthesis

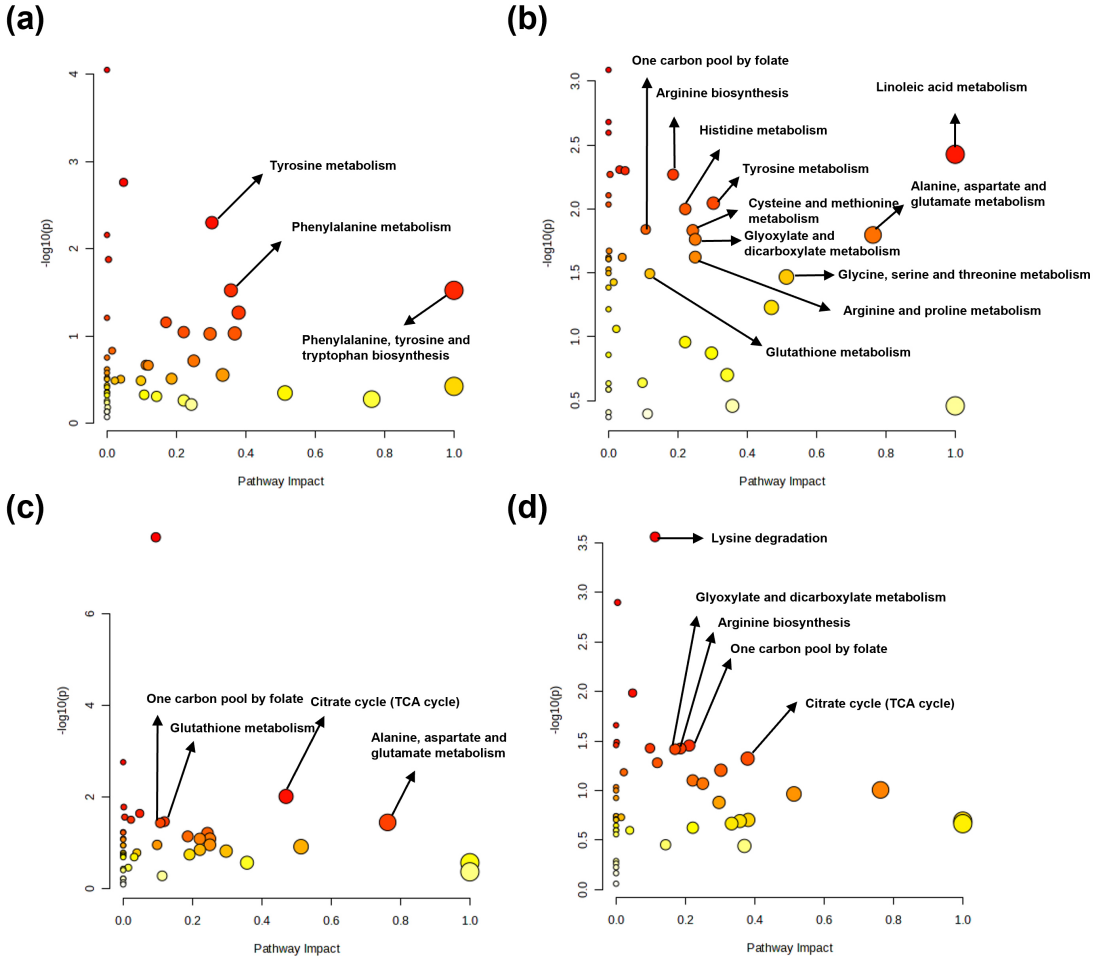

Fig. 6. Metabolic pathway analysis of determined metabolites in tissues from control and sepsis mice. Major metabolic pathways identified from determined metabolites in the (a) kidney, (b) spleen, (c) lung, and (d) liver.

from ornithine rather than methionine salvage, as methionine levels show only a decreasing trend [43,44]. Uridine and adenosine, markers of RNA turnover and ATP degradation, respectively, were elevated in the lungs but not in other organs. This indicates preserved pulmonary function and metabolic activity despite systemic inflammation. The TCA cycle intermediates succinic acid and *cis*-aconitic acid were decreased in the lungs but elevated in the kidney and spleen, suggesting intact mitochondrial function in the lungs. Correspondingly, lower lactic acid levels in the lungs support efficient oxidative metabolism, which may contribute to relative functional preservation and favorable prognosis in sepsis [45]. Consistent with our lung findings, a clinical targeted-metabolomics study in sepsis-induced acute respiratory distress syndrome (ARDS) reported broad disturbances in amino-acid and lipid pathways that discriminated ARDS from non-ARDS and also separated direct from indirect ARDS subphenotypes [46]. Together with the decreases in lactate, succinic acid, and cis-aconitic acid observed in our lung tissue, these data point toward sepsis-related rewiring of central carbon metabolism within the pulmonary compartment, with potential links to mitochondrial dysfunction. While tissue-level changes cannot be directly equated to circulating biomarkers, the convergence of tissue and serum signatures suggests a translational bridge worth testing in future studies.

In liver tissue, seven metabolites (α-aminobutyric acid, pipecolic acid, uridine, inosine, adenosine, glycolic acid, and oxaloacetic acid) were identified as potential biomarkers indicative of sepsis-induced hepatic injury. α-Aminobutyric acid is derived from methionine and lysine metabolism via two routes: the pipecolate and saccharopine pathways, both branching from α-aminoadipic semialdehyde [47]. In this study, elevated α-aminobutyric acid, alongside detectable pipecolic acid, in the liver suggests that under septic conditions, lysine catabolism preferentially proceeds via the pipecolate pathway. Normally, the saccharopine pathway dominates, and pipecolic acid remains low [41]; however, its abnormal accumulation has been linked to oxidative stress and tissue damage in multiple organs, including the liver [48,49]. Thus, the activation of the pipecolate pathway may contribute to liver and spleen dysfunction in sepsis. The reductions in uridine and adenosine levels likely resulted from increased nucleoside con-

sumption and impaired regeneration under inflammatory and metabolic stress. In particular, the ROS molecules generated during sepsis suppress glutamine synthetase and activate xanthine oxidase, which promotes the degradation of inosine to uric acid [50–52]. This cascade may represent a compensatory antioxidant response but also reflects heightened nucleotide catabolism. Decreased glycolic acid, oxaloacetic acid, and malonic acid levels suggested disrupted hepatic glucose and lipid metabolism. The glyoxylate cycle, which is primarily active in the liver peroxisomes, may be involved in alternative gluconeogenesis [53]. The reduction in malonic acid, a known TCA cycle inhibitor [54], and oxaloacetic acid may indicate increased metabolic flux through the TCA cycle during sepsis.

Multi-omics investigations could mechanistically anchor our organ-specific signatures to energy pathways. In a sequential renal biopsy model of experimental sepsis, early and stepwise impairments in oxidative phosphorylation with increased uncoupling were documented prior to macro-hemodynamic alterations [24]. Recent reviews further emphasize that metabolic reprogramming particularly a shift toward glycolysis with suppression of fatty-acid oxidation drives injury and recovery trajectories in AKI [55]. Therefore, the metabolites identified in this study may serve as potential biomarkers for the early diagnosis of sepsis-induced organ-specific injuries. These findings are expected to provide an important foundation for prognosis prediction and the development of personalized therapeutic strategies for patients with sepsis.

5. Conclusions

In this study, targeted metabolomic analysis was conducted on kidney, spleen, lung, and liver tissues of a mouse model of sepsis to characterize organ-specific metabolic alterations and identify potential biomarkers indicative of sepsis-induced organ injury. A total of 29 metabolites were selected through statistical and pathway analyses that revealed distinct metabolic changes specific to each organ. Notably, four metabolites in the kidney (tyrosine, epinephrine, 5-hydroxytryptophan, and kynurenic acid), 10 metabolites in the spleen (including serine, 4-hydroxyproline, normetanephrine, xanthosine, uridine, adenosine, succinic acid, *cis*-aconitic acid, linoleic acid, and eicosadienoic acid), 8 metabolites in the lung (such as alanine, α-aminobutyric acid, ornithine, uridine, adenosine, 5-MTA, succinic acid, and *cis*-aconitic acid), and 7 metabolites in the liver (such as α-aminobutyric acid, pipecolic acid, uridine, inosine, adenosine, glycolic acid, and oxaloacetic acid) were identified as potential biomarkers that may reflect organ-specific metabolic alterations associated with sepsis. These findings reflect the organ-specific metabolic responses to sepsis and suggest that the identified metabolites may serve as potential biomarkers for early diagnosis and prognosis prediction. This study provides a foundation for future efforts aimed at precision diagnostics and the development of personalized therapeutic strategies for patients with sepsis.

Abbreviations

LC–MS/MS, Liquid chromatography-tandem mass spectrometry; GC–MS/MS, Gas chromatography-tandem mass spectrometry; PCA, Principal component analysis; PLS-DA, partial least squares discriminant analysis; MTA, 5′-deoxy-5′methylthioadenosine; AA, Amino acid; OA, Organic acid; FA, Fatty acid; NSs, Nucleosides; KPs, Kynurenine pathway metabolites; IS, Internal standard; EOC, Ethoxycarbonylation; TBDMS, *Tert*-butyldimethylsilylation; MO, Methoximation; ECF, Ethylchloroformate; MTBSTFA, N-Methyl-N-(tert-butyldimethylsilyl) trifluoroacetamide; PCA, Principal component analysis; PLS-DA, Partial least square discriminant analysis; VIP, Variable importance in projection; TCA, Tricarboxylic acid; IDO, 2,3-Dioxygenase; ATP, Adenosine triphosphate; ROS, Reactive oxygen species.

Availability of Data and Materials

The data presented in this study are contained in this article/supplementary material or available upon request from the corresponding author.

Author Contributions

MJP designed the study, wrote, edited the manuscript, and supervised the study. MJ and BC performed sample preparation and analysis and wrote the manuscript. CK and JL performed the sample collection and sample preparation. All authors contributed to editorial changes in the manuscript. All authors read and approved the final manuscript. All authors have participated sufficiently in the work and agreed to be accountable for all aspects of the work.

Ethics Approval and Consent to Participate

All animal experiments were conducted at Konkuk University in accordance with the ARRIVE guidelines as well as the institutional guidelines of the Institutional Animal Care and Use Committee (IACUC) of Konkuk University (approval number: KU17044-2).

Acknowledgment

We thank Dr. In Duk Jung of Konkuk University for providing search materials for this study.

Funding

This study was supported by a National Research Foundation of Korea (NRF) grant funded by the Ministry of Education, Science, and Technology (2023R1A2C1003696).

Conflict of Interest

The authors declare no conflict of interest.

Supplementary Material

Supplementary material associated with this article can be found, in the online version, at https://doi.org/10.31083/FBL45558.

References

[1] Matot I, Sprung CL. Definition of sepsis. Intensive Care Medicine. 2001; 27 Suppl 1: S3–S9. https://doi.org/10.1007/pl00003795.

[2] Li Y, Wang C, Chen M. Metabolomics-based study of potential biomarkers of sepsis. Scientific Reports. 2023; 13: 585. https://doi.org/10.1038/s41598-022-24878-z.

[3] Liu YC, Yao Y, Yu MM, Gao YL, Qi AL, Jiang TY, *et al*. Frequency and mortality of sepsis and septic shock in China: a systematic review and meta-analysis. BMC Infectious Diseases. 2022; 22: 564. https://doi.org/10.1186/s12879-022-07543-8.

[4] van der Poll T, van de Veerdonk FL, Scicluna BP, Netea MG. The immunopathology of sepsis and potential therapeutic targets. Nature Reviews. Immunology. 2017; 17: 407–420. https://doi.org/10.1038/nri.2017.36.

[5] Evans L, Rhodes A, Alhazzani W, Antonelli M, Coopersmith CM, French C, *et al*. Surviving sepsis campaign: international guidelines for management of sepsis and septic shock 2021. Intensive Care Medicine. 2021; 47: 1181–1247. https://doi.org/10.1007/s00134-021-06506-y.

[6] Pierrakos C, Velissaris D, Bisdorff M, Marshall JC, Vincent JL. Biomarkers of sepsis: time for a reappraisal. Critical Care (London, England). 2020; 24: 287. https://doi.org/10.1186/s13054-020-02993-5.

[7] He RR, Yue GL, Dong ML, Wang JQ, Cheng C. Sepsis Biomarkers: Advancements and Clinical Applications-A Narrative Review. International Journal of Molecular Sciences. 2024; 25: 9010. https://doi.org/10.3390/ijms25169010.

[8] Wang X, Li R, Qian S, Yu D. Multilevel omics for the discovery of biomarkers in pediatric sepsis. Pediatric Investigation. 2023; 7: 277–289. https://doi.org/10.1002/ped4.12405.

[9] Fujishima S. Organ dysfunction as a new standard for defining sepsis. Inflammation and Regeneration. 2016; 36: 24. https://doi.org/10.1186/s41232-016-0029-y.

[10] Wang X, Huang P, Luo Y, Xin Y, Li Y, Shen L, *et al*. Urinary 3-methylhistidine as a potential biomarker for sepsis-associated acute kidney injury: multidimensional metabolomics analysis in mice and human. Annals of Intensive Care. 2025; 15: 125. https://doi.org/10.1186/s13613-025-01550-z.

[11] Huang P, Liu Y, Li Y, Xin Y, Nan C, Luo Y, *et al*. Metabolomics- and proteomics-based multi-omics integration reveals early metabolite alterations in sepsis-associated acute kidney injury. BMC Medicine. 2025; 23: 79. https://doi.org/10.1186/s12916-025-03920-7.

[12] Nian W, Tao W, Zhang H. Review of research progress in sepsis-associated acute kidney injury. Frontiers in Molecular Biosciences. 2025; 12: 1603392. https://doi.org/10.3389/fmolb.2025.1603392.

[13] McCann MR, Fry C, Maile MD, Farkash EA, Cummings BC, Flott TL, *et al*. Early Sepsis Metabolic Changes in Kidney and Liver Precede Clinical Evidence of Organ Dysfunction. American Journal of Respiratory Cell and Molecular Biology. 2025; 73: 299–309. https://doi.org/10.1165/rcmb.2024-0391OC.

[14] Beckonert O, Keun HC, Ebbels TMD, Bundy J, Holmes E, Lindon JC, *et al*. Metabolic profiling, metabolomic and metabonomic procedures for NMR spectroscopy of urine, plasma, serum and tissue extracts. Nature Protocols. 2007; 2: 2692–2703. https://doi.org/10.1038/nprot.2007.376.

[15] Hussain H, Vutipongsatorn K, Jiménez B, Antcliffe DB. Patient Stratification in Sepsis: Using Metabolomics to Detect Clinical Phenotypes, Sub-Phenotypes and Therapeutic Response. Metabolites. 2022; 12: 376. https://doi.org/10.3390/metabo12050376.

[16] Changsirivathanathamrong D, Wang Y, Rajbhandari D, Maghzal GJ, Mak WM, Woolfe C, *et al*. Tryptophan metabolism to kynurenine is a potential novel contributor to hypotension in human sepsis. Critical Care Medicine. 2011; 39: 2678–2683. https://doi.org/10.1097/CCM.0b013e31822827f2.

[17] Ji M, Lee HS, Kim Y, Seo C, Oh S, Jung ID, *et al*. Metabolomic Study of Normal and Modified Nucleosides in the Urine of Mice with Lipopolysaccharide-Induced Sepsis by LC–MS/MS. Bulletin of the Korean Chemical Society. 2021; 42: 611–617. https://doi.org/10.1002/bkcs.12240.

[18] Lee SJ, Gharbi A, You JS, Han HD, Kang TH, Hong SH, *et al*. Drug repositioning of TANK-binding kinase 1 inhibitor CYT387 as an alternative for the treatment of Gram-negative bacterial sepsis. International Immunopharmacology. 2019; 73: 482–490. https://doi.org/10.1016/j.intimp.2019.05.051.

[19] Choi B, Ji M, Oh S, Kim Y, Choi S, Kim HW, *et al*. Aged Brain Metabolomics Study by Metabolic Profiling Analysis of Amino Acids, Organic Acids, and Fatty Acids in Cortex, Cerebellum, Hypothalamus, and Hippocampus of Rats. Frontiers in Bioscience (Landmark Edition). 2024; 29: 306. https://doi.org/10.31083/j.fbl2908306.

[20] Su L, Li H, Xie A, Liu D, Rao W, Lan L, *et al*. Dynamic changes in amino acid concentration profiles in patients with sepsis. PloS One. 2015; 10: e0121933. https://doi.org/10.1371/journal.pone.0121933.

[21] Conlay LA, Maher TJ, Wurtman RJ. Tyrosine accelerates catecholamine synthesis in hemorrhaged hypotensive rats. Brain Research. 1985; 333: 81–84. https://doi.org/10.1016/0006-8993(85)90126-x.

[22] Zeden JP, Fusch G, Holtfreter B, Schefold JC, Reinke P, Domanska G, *et al*. Excessive tryptophan catabolism along the kynurenine pathway precedes ongoing sepsis in critically ill patients. Anaesthesia and Intensive Care. 2010; 38: 307–316. https://doi.org/10.1177/0310057X1003800213.

[23] Xiang L, Wanli M, Jiannan S, Zhanfei H, Qi Z, Haibo L. To explore the molecular mechanism of IRF7 involved in acute kidney injury in sepsis based on proteomics. Proteome Science. 2025; 23: 6. https://doi.org/10.1186/s12953-025-00244-5.

[24] Müller J, Chvojka J, Ledvinova L, Benes J, Tuma Z, Grundmanova M, *et al*. Renal mitochondria response to sepsis: a sequential biopsy evaluation of experimental porcine model. Intensive Care Medicine Experimental. 2025; 13: 25. https://doi.org/10.1186/s40635-025-00732-0.

[25] Rodriguez AE, Ducker GS, Billingham LK, Martinez CA, Mainolfi N, Suri V, *et al*. Serine Metabolism Supports Macrophage IL-1β Production. Cell Metabolism. 2019; 29: 1003–1011.e4. https://doi.org/10.1016/j.cmet.2019.01.014.

[26] Xu LL, Zhou Z, Schäuble S, Vivas W, Dlubatz K, Bauer M, *et al*. Multi-Omics and -Organ Insights into Energy Metabolic Adaptations in Early Sepsis Onset. Advanced Science (Weinheim, Baden-Wurttemberg, Germany). 2025; 12: e04418. https://doi.org/10.1002/advs.202504418.

[27] Efron ML, Bixby EM, Hockaday TD, Smith LH, Jr, Meshorer E. Hydroxyprolinemia. 3. The origin of free hydroxyproline in hydroxyprolinemia. Collagen turnover. Evidence for biosynthetic pathway in man. Biochimica et Biophysica Acta. 1968; 165: 238–250. https://doi.org/10.1016/0304-4165(68)90052-4.

[28] Hahn PY, Wang P, Tait SM, Ba ZF, Reich SS, Chaudry IH. Sustained elevation in circulating catecholamine levels during

polymicrobial sepsis. Shock (Augusta, Ga.). 1995; 4: 269–273. https://doi.org/10.1097/00024382-199510000-00007.

[29] Hoover DB, Brown TC, Miller MK, Schweitzer JB, Williams DL. Loss of Sympathetic Nerves in Spleens from Patients with End Stage Sepsis. Frontiers in Immunology. 2017; 8: 1712. https://doi.org/10.3389/fimmu.2017.01712.

[30] Galley HF, Davies MJ, Webster NR. Xanthine oxidase activity and free radical generation in patients with sepsis syndrome. Critical Care Medicine. 1996; 24: 1649–1653. https://doi.org/10.1097/00003246-199610000-00008.

[31] Ramos MFDP, Monteiro de Barros ADCM, Razvickas CV, Borges FT, Schor N. Xanthine oxidase inhibitors and sepsis. International Journal of Immunopathology and Pharmacology. 2018; 32: 2058738418772210. https://doi.org/10.1177/2058738418772210.

[32] Lovászi M, Németh ZH, Gause WC, Beesley J, Pacher P, Haskó G. Inosine monophosphate and inosine differentially regulate endotoxemia and bacterial sepsis. FASEB Journal: Official Publication of the Federation of American Societies for Experimental Biology. 2021; 35: e21935. https://doi.org/10.1096/fj.202100862R.

[33] Milne GR, Palmer TM. Anti-inflammatory and immunosuppressive effects of the A2A adenosine receptor. TheScientificWorldJournal. 2011; 11: 320–339. https://doi.org/10.1100/tsw.2011.22.

[34] Lai K, Song C, Gao M, Deng Y, Lu Z, Li N, *et al*. Uridine Alleviates Sepsis-Induced Acute Lung Injury by Inhibiting Ferroptosis of Macrophage. International Journal of Molecular Sciences. 2023; 24: 5093. https://doi.org/10.3390/ijms24065093.

[35] Li G, Hu Y, Xu F, Li F. Uridine-mediated Activation of the Keap1-Nrf2 Pathway for Alleviating Sepsis-induced Acute Lung Injury. Pharmacognosy Magazine. 2024; 21: 650–661. https://doi.org/10.1177/09731296241275755.

[36] Ilias I, Vassiliadi DA, Theodorakopoulou M, Boutati E, Maratou E, Mitrou P, *et al*. Adipose tissue lipolysis and circulating lipids in acute and subacute critical illness: effects of shock and treatment. Journal of Critical Care. 2014; 29: 1130.e5–1130.e9. https://doi.org/10.1016/j.jcrc.2014.06.003.

[37] Choi SM, Tucker DF, Gross DN, Easton RM, DiPilato LM, Dean AS, *et al*. Insulin regulates adipocyte lipolysis via an Akt-independent signaling pathway. Molecular and Cellular Biology. 2010; 30: 5009–5020. https://doi.org/10.1128/MCB.00797-10.

[38] Lanza-Jacoby S, Tabares A. Triglyceride kinetics, tissue lipoprotein lipase, and liver lipogenesis in septic rats. The American Journal of Physiology. 1990; 258: E678–E685. https://doi.org/10.1152/ajpendo.1990.258.4.E678.

[39] Mauvoisin D, Mounier C. Hormonal and nutritional regulation of SCD1 gene expression. Biochimie. 2011; 93: 78–86. https://doi.org/10.1016/j.biochi.2010.08.001.

[40] Tan TL, Goh YY. The role of group IIA secretory phospholipase A2 (sPLA2-IIA) as a biomarker for the diagnosis of sepsis and bacterial infection in adults-A systematic review. PloS One. 2017; 12: e0180554. https://doi.org/10.1371/journal.pone.0180554.

[41] Hallen A, Jamie JF, Cooper AJL. Lysine metabolism in mammalian brain: an update on the importance of recent discoveries. Amino Acids. 2013; 45: 1249–1272. https://doi.org/10.1007/s00726-013-1590-1.

[42] Oh TS, Zabalawi M, Jain S, Long D, Stacpoole PW, McCall CE, *et al*. Dichloroacetate improves systemic energy balance and feeding behavior during sepsis. JCI Insight. 2022; 7: e153944. https://doi.org/10.1172/jci.insight.153944.

[43] Noguchi Y, Meyer TA, Tiao G, Ogle CK, Fischer JE, Hasselgren PO. Influence of sepsis and endotoxemia on polyamine metabolism in mucosa of small intestine in rats. Metabolism: Clinical and Experimental. 1996; 45: 28–33. https://doi.org/10.1016/s0026-0495(96)90196-1.

[44] Hevia H, Varela-Rey M, Corrales FJ, Berasain C, Martínez-Chantar ML, Latasa MU, *et al*. 5′-methylthioadenosine modulates the inflammatory response to endotoxin in mice and in rat hepatocytes. Hepatology (Baltimore, Md.). 2004; 39: 1088–1098. https://doi.org/10.1002/hep.20154.

[45] Wang Z, Gao H, Ma X, Zhu D, Zhao L, Xiao W. Adrenic acid: A promising biomarker and therapeutic target (Review). International Journal of Molecular Medicine. 2025; 55: 20. https://doi.org/10.3892/ijmm.2024.5461.

[46] Chang Y, Yoo HJ, Kim SJ, Lee K, Lim CM, Hong SB, *et al*. A targeted metabolomics approach for sepsis-induced ARDS and its subphenotypes. Critical Care (London, England). 2023; 27: 263. https://doi.org/10.1186/s13054-023-04552-0.

[47] Struys EA, Jakobs C. Metabolism of lysine in alpha-aminoadipic semialdehyde dehydrogenase-deficient fibroblasts: evidence for an alternative pathway of pipecolic acid formation. FEBS Letters. 2010; 584: 181–186. https://doi.org/10.1016/j.febslet.2009.11.055.

[48] Armstrong DW, Gasper M, Lee SH, Zukowski J, Ercal N. D-amino acid levels in human physiological fluids. Chirality. 1993; 5: 375–378. https://doi.org/10.1002/chir.530050519.

[49] Somaio Neto F, Ikejiri AT, Bertoletto PR, Chaves JCB, Teruya R, Fagundes DJ, *et al*. Gene expression related to oxidative stress in the heart of mice after intestinal ischemia. Arquivos Brasileiros De Cardiologia. 2014; 102: 165–173. https://doi.org/10.5935/abc.20130240.

[50] Rapisarda A, Pastorino S, Massazza S, Varesio L, Bosco MC. Antagonistic effect of picolinic acid and interferon-gamma on macrophage inflammatory protein-1alpha/beta production. Cellular Immunology. 2002; 220: 70–80. https://doi.org/10.1016/s0008-8749(03)00008-x.

[51] Pinteaux E, Copin JC, Ledig M, Tholey G. Modulation of oxygen-radical-scavenging enzymes by oxidative stress in primary cultures of rat astroglial cells. Developmental Neuroscience. 1996; 18: 397–404. https://doi.org/10.1159/000111433.

[52] Bleisch S, Sillero MA, Torrecilla A, Sillero A. Uric acid synthesis by rat liver supernatants from purine bases, nucleosides and nucleotides. Effect of allopurinol. Cell Biochemistry and Function. 1994; 12: 237–245. https://doi.org/10.1002/cbf.290120403.

[53] Liaudet L, Mabley JG, Soriano FG, Pacher P, Marton A, Haskó G, *et al*. Inosine reduces systemic inflammation and improves survival in septic shock induced by cecal ligation and puncture. American Journal of Respiratory and Critical Care Medicine. 2001; 164: 1213–1220. https://doi.org/10.1164/ajrccm.164.7.2101013.

[54] Kim YS. Malonate metabolism: biochemistry, molecular biology, physiology, and industrial application. Journal of biochemistry and molecular biology. 2002; 35: 443–451. https://doi.org/10.5483/bmbrep.2002.35.5.443.

[55] Cao M, Zhao X, Xia F, Shi M, Zhao D, Li L, *et al*. Mitochondrial dysfunction and metabolic reprogramming in acute kidney injury: mechanisms, therapeutic advances, and clinical challenges. Frontiers in Physiology. 2025; 16: 1623500. https://doi.org/10.3389/fphys.2025.1623500.